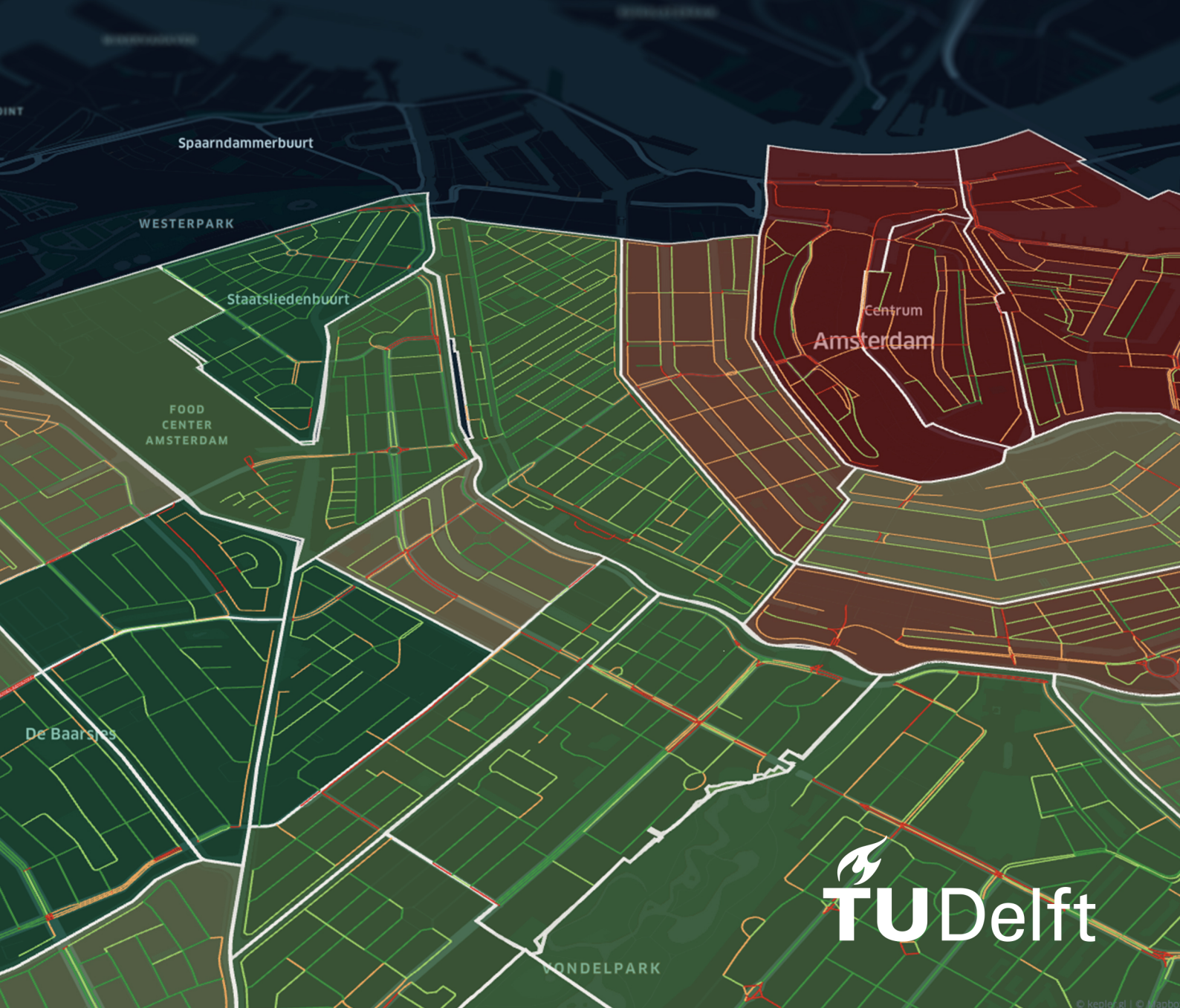


Measuring Natural Surveillance at Scale

An Automated Method for Investigating the Relation Between the ‘Eyes on the Street’ and Urban Safety

Timo van Asten



Measuring Natural Surveillance at Scale

An Automated Method for Investigating the Relation Between the 'Eyes on the Street' and Urban Safety

by

Timo van Asten

to obtain the degree of Master of Science
at the Delft University of Technology,
to be defended publicly on Wednesday December 8, 2021 at 12:00.

Student number: 4485270
Thesis committee:
Chair Prof. dr. ir. A. Bozzon, TU Delft
Daily supervisor Dr. A. Psyllidis, TU Delft
Committee member Dr. P. Pawełczak, TU Delft

An electronic version of this thesis is available at <http://repository.tudelft.nl/>.



Abstract

To create safe urban areas, it is important to gain insight into what influences the (perceived) safety of our cities and human settlements. One of the factors that can contribute to safety is the way urban spaces are designed. Previous work has highlighted the importance of *natural surveillance*: a type of surveillance that is a byproduct of how citizens normally and routinely use the environment. However, studying this concept is not a trivial task. Manual approaches such as observation studies are costly and time consuming and have therefore often limited themselves to smaller geographical areas.

In this work, we present a methodology that can automatically provide an estimate of natural surveillance by detecting building openings (i.e. windows and doors) in street level imagery and localizing them in 3 dimensions. The proposed method is able to estimate natural surveillance at the street segment level, while simultaneously being able to gather data on a whole city in a matter of hours. We then apply our method to the city of Amsterdam to analyze the relationship between natural surveillance and urban safety using the Amsterdam Safety Index.

We conclude that our chosen operationalization of natural surveillance (road surveillability and occupant surveillability) is correlated with decreases in high impact crime and nuisance as well as increases in perceived safety. Furthermore we provide evidence for the existence of a threshold after which extra natural surveillance is no longer associated with higher degrees of safety.

Preface

The work that lies before you, is one that, quite literally, is about everyone's look at the world. It is a work that investigates how we might keep each other safe, without even noticing, by doing something as simple as looking out of your window.

This is exactly what drew me to studying this topic: *natural surveillance*. I loved how I could have interesting discussions about it with everyone I explained it to, since it is a concept everybody can get a grasp of.

Writing this work has been quite a challenge at times, especially when we were locked inside, looking outside onto empty streets. This is why I want to especially thank Robbert and Nick. Working on our theses together during the COVID-19 lockdowns kept me going and made it a fun endeavor.

I want to furthermore thank everyone that has provided input into this work and who have helped me towards producing something I can be proud of: my supervisors Achilleas and Alessandro for guiding me during this research journey, Samuel Langton from the NSCR for his helpful perspective and interesting discussions about my work, my family and friends for keeping me going and my girlfriend Irem for kicking me over the finish line.

This work will also mark the end of my journey at the TU Delft. It has been a hell of a ride which I will never forget. One that has taken me all over the world, from the US to Japan, made me build a vehicle that went faster than a F1 car and has enriched my life with knowledge, friendships and experiences that will remain in my heart forever.

I hope you will enjoy the work and wish you a pleasant read :)

*Timo van Asten
Delft, November 2021*

*In memoriam of opa Jan
† August 3, 2021*

Contents

1	Introduction	1
1.1	Context and Background	1
1.2	Problem.	1
1.3	Objective and Research Questions	1
1.4	Methodology	2
1.5	Contributions.	2
2	Related Work	3
2.1	Natural Surveillance	3
2.1.1	"Eyes on the Street"	3
2.1.2	Defensible Space Theory.	4
2.1.3	Crime Prevention Through Environmental Design (CPTED)	4
2.2	Operationalizing Natural Surveillance	4
2.2.1	Manual Approaches	5
2.2.2	Computational Approaches	6
3	Methodology	9
3.1	Selected Features	9
3.2	Data Pipeline	9
3.2.1	Data Collection	9
3.2.2	Data Processing	13
3.2.3	Calculating Road Surveillability and Occupant Surveillability	16
3.3	Evaluation	19
3.3.1	Previous Evaluations of Used Algorithms	19
3.3.2	Evaluation of Building Opening Geolocation.	21
4	Experiment Design	25
4.1	Amsterdam Safety Index	25
4.1.1	Datasources	25
4.1.2	Composition of the Index	27
4.2	Applying Our Methodology to Amsterdam	29
4.2.1	Included Neighborhoods	29
4.2.2	Hardware and Software	29
4.2.3	Data Collection	29
4.2.4	Calculating Road Surveillability and Occupant Surveillability	29
4.2.5	Correlation with the Amsterdam Safety Index	30
5	Results	33
5.1	Road Surveillability	33
5.2	Occupant Surveillability	33
5.3	Manual Assessment.	34
6	Discussion	45
6.1	Discussion of Experiment Results.	45
6.1.1	Differences in Included Floor Levels and Sightline Lengths	45
6.1.2	Differences Between the 2019 and 2020 Safety Index.	46
6.1.3	Non-linear Relationship	46
6.2	Discussion of the Methodology	46
6.2.1	Ability to Capture the Notion Natural Surveillance at Scale.	46
6.2.2	Technical Limitations	48
6.3	Availability of Code and Data	48

7 Conclusion	49
7.1 Main Findings.	49
7.1.1 Measuring Natural Surveillance in a Scalable Way	49
7.1.2 Relationship Between Natural Surveillance and Safety.	50
7.2 Future Work.	50
Bibliography	51

1

Introduction

1.1. Context and Background

Crime and the fear of it are fundamental problems in all communities. At the same time, the world is urbanizing at a fast pace. In 2018, more than half of the world's population lived in an urban area and it is predicted that over two thirds of the world's population will do so by 2050 [51]. It is therefore that making cities and human settlements safe is one of the key aspirations of the 2030 Agenda of the United Nations [50]. To achieve this goal, it is important to understand what makes the spaces we live in both be safe and feel safe. One of the many aspects that can contribute to safety is the way urban spaces are designed. Since the 1960's multiple theories have been proposed how these spaces can be designed in a way that increases safety, such as those in Jane Jacobs' book *The Death and Life of Great American Cities* [22], Oscar Newman's defensible space theory [38] and more recently, Crime Prevention Through Environmental Design (CPTED) [12].

Something all these theories have in common is that they highlight the importance of *natural surveillance*¹: a type of surveillance that is a byproduct of how citizens normally and routinely use the environment [12]. There are a multitude of factors that can influence this type of surveillance, like good lighting and the presence of unobstructed windows overlooking an area. Such attributes have shown an inverse relationship with the incidence of crime [16, 29] and designing urban spaces in a way that enhances natural surveillance has been adopted as a guideline by the United Nations Human Settlements Programme [50].

1.2. Problem

To study the importance of natural surveillance in creating safe urban spaces, it is important that it can be measured in some way. Given the scale and diversity of cities, this is not a trivial task. Natural surveillance has previously been studied by manually collecting data through observation studies, either in real life or virtually. Examples include letting participants judge how well an area could be observed [16, 28, 29, 42, 43], looking at the presence of certain building features that increase visibility, like front porches and balconies [16] or by manually constructing models of the environment to calculate possible sightlines [1].

Such methods, however, are time consuming and costly. For example, a 2020 study by Amiri [1] that analyzed sightlines for 3179 building openings (i.e. windows and doors) stated that collecting and georeferencing spatial data for the study took approximately 1 year to complete with 8 hours a day, 5 days a week. Consequently, these studies restrict themselves to smaller geographical areas like (part of) a neighborhood. Although such research can give us valuable insights, this limitation makes it hard to generalize them to other neighborhoods, cities and countries.

1.3. Objective and Research Questions

To overcome this problem of scale, measuring natural surveillance in an automated fashion presents itself as a logical solution. However, previous research that attempts this does so by using very basic features of

¹Other terms used for this concept are "eyes on the street" and informal surveillance.

the environment that act as a proxy for visibility onto the street, such as the distance between buildings [13, 46].

Using such an operationalization loses many subtle details that can effect natural surveillance, such as where in the building windows are present and if those windows are blocked by fencing or vegetation. Aim of this work will be to improve upon such methodologies. Furthermore it aims to provide meaning to the data that can be collected by such a methodology by juxtaposing it to real life data on urban safety and investigating what can be learned from it. This leads us to the following research questions:

RQ1 How can the notion of natural surveillance be measured in a scalable way?

RQ2 How do the measurements produced by the proposed methodology relate to the (perceived) safety of an urban area?

1.4. Methodology

In this day and age, more and more data is being collected in our cities. At the same time, advancements in computer vision and machine learning techniques are providing the tools needed to extract more detailed information from such data sources. Street level imagery has previously shown to be a reliable way to perform observation studies [4, 28, 39, 41]. In previous research, street level imagery in combination with computer vision has shown to be an effective tool to assess all sorts of aspects of the cities we live in, like classifying land use, predicting urban safety and monitoring camera surveillance in urban areas. [21, 49]. This indicates that such tools could be used to create a methodology to measure natural surveillance in a way that is both scalable to the city level, yet is able of capturing some of its nuances at the street level.

For answering **RQ1**: 'How can the notion of natural surveillance be measured in a scalable way?', we review previous literature on natural surveillance, and, based on this work, select two features to include in the operationalization:

- **Road surveillability:** the surveillability of building openings from the streets and vice versa.
- **Occupant surveillability:** the surveillability of building openings by other neighboring building openings.

Next, we consider what is needed to calculate these features at scale and construct a data pipeline which is capable of doing so. The pipeline takes a geographical area as input and automatically retrieves building footprints and street view imagery of building facades. It then uses recently developed facade labeling and geolocation algorithms [30, 41] to detect and localize building openings within the urban area of interest. From these localized building openings, we then calculate possible sightlines from building openings onto the street and other building openings as a measure for the two features outlined above.

For answering **RQ2**: 'How do the measurements produced by the proposed methodology relate to the (perceived) safety of an urban area?', we calculate the two features for a multitude of neighborhoods throughout Amsterdam and correlate them with a safety index published by the municipality [2] comprised of crime reports and neighborhood surveys on the (perceived) safety of 104 neighborhoods.

1.5. Contributions

Our main contributions are as follows:

- We present a methodology to collect data on natural surveillance in a scalable way.
- We deploy the methodology on the city of Amsterdam and analyze the obtained data to investigate the influence of natural surveillance on (perceived) safety.
- We share the obtained data as a new dataset. Such data could, for example, be used for further research into natural surveillance, assist in deciding where other forms of surveillance such as police patrols or CCTV are most needed or could serve as new input for crime prediction models.

2

Related Work

2.1. Natural Surveillance

Natural surveillance is a concept that is part of multiple frameworks that aim of deter crime by altering the built environment. To give the context in which to view natural surveillance, this section will introduce these frameworks and how they came to be. Furthermore it will explain what natural surveillance is and what previous research has shown about the effects of natural surveillance on safety and the feeling of safety.

2.1.1. "Eyes on the Street"

In 1961, Jane Jacobs published her book *The Death and Life of Great American Cities* [22]. In this book she critiqued the modernist urban planning practices of the 1950s, which according to her oversimplified the complexity of human activities within cities. She is commonly accredited with creating focus for elements of safety which could be facilitated by design, management and use of the urban environment [10]. According to Jacobs, city streets that could turn the presence of strangers into a safety asset had to possess the following qualities:

1. A clear demarcation between what is public space and what is private space.
2. There should be *eyes upon the street*, belonging to what she called the *natural proprietors* of the street. Buildings should be oriented towards the street to make them insure the safety of both the residents and strangers on the street.
3. Sidewalks should have fairly continuous stream of people on them. Both to add to the effective number of eyes on the street and to induce people in buildings to watch the sidewalks, observing how 'large numbers of people entertain themselves, off and on, by watching street activity'.

These ideas became collectively known under the name: 'eyes on the street'. While these aims seem simple, Jacobs stated that achieving them was not as simple since '[y]ou can't make people use streets they have no reason to use', and '[y]ou can't make people watch streets they do not want to watch'. Jacobs argued that 'eyes on the street' could be promoted through mixed land uses. Mixing a substantial quantity of stores and other public places along the sidewalks of a district would increase safety for multiple reasons:

1. It would give people reasons to use the streets,
2. It would draw people from other areas thus populating those streets as well.
3. Store owners themselves are, according to Jacobs, great street watchers when present in sufficient numbers since they do not want their customers to be nervous about safety.
4. The activity caused by people on errands or looking for food and/or drinks would attract other users.

The key take away here is that Jacobs argued that by designing cities in such a way that people are always watching and being watched, citizens will keep each other safe. However, many of the assertions Jacobs made about crime were based on anecdotal observation and were not backed up by systematically recorded crime data to support them [10].

2.1.2. Defensible Space Theory

Building upon the ideas of Jacobs, Oscar Newman introduced Defensible Space Theory [38] in 1972. His theory can be described as "a system through which crime can be prevented by increasing the opportunities for residents to control and defend their space against crime, while simultaneously eliminating physical characteristics that attract offenders" [44]. It consists of three main components [38]:

1. **Territoriality:** "the capacity of the physical environment to create perceived zones of territorial influences."
2. **Milieu and image:** "the capacity of design to influence the perception of a project's uniqueness, isolation, and stigma."
3. **Natural surveillance:** "the capacity of physical design to provide surveillance opportunities for residents and their agents."

It is in this theory we first see the term *natural surveillance*, which is clearly very similar to Jacobs' "*eyes on the street*". Both terms are still used today, but in this work we will use to the term natural surveillance to refer to this concept.

Newman puts forward that windows and doors that are facing each other would provide better visibility of the private and public space around residences. Having buildings face each other and overlook public spaces, would increase the probability that potential offenders would be spotted or caught in the act. Furthermore, he states that lines of sight from residences should be clear and unobstructed to make it possible for residents to have a good overview of the area. The increased sense of security generated by natural surveillance would also result in more frequent use of space by residents, increasing their desire to defend that space.

2.1.3. Crime Prevention Through Environmental Design (CPTED)

Over the next decades Newman's Defensible Space theory would be refined and extended by him and others, like Timothy D. Crowe, to a field that is now known as Crime Prevention Through Environmental Design or CPTED (pronounced 'sep-ted'). Many of the same concepts still remain. Crowe describes CPTED as consisting of three overlapping strategies: territorial reinforcement, natural access control and natural surveillance, with the latter two being the main focus of physical design programs [12].

CPTED has received support by the United Nations [50] and by governments all around the world including the United States, Canada, the United Kingdom, Australia, New Zealand, and throughout Europe, South America and Asia [11]. The ideas of CPTED have also been adopted by law enforcement in programs such as Secured by Design¹ in the UK and Politie Keurmerk Veilig Wonen² in the Netherlands.

Regarding natural surveillance, there are a multitude of changes that can be made to the environment to increase natural surveillance. These include [12]:

- Installing windows in the dead walls on the sides of buildings.
- Removing walls and hedges that impede natural surveillance.
- Incentivizing people to use the outdoor space, for example with porches, yards and gardening.
- Preventing light pollution on bedroom windows such that residents will be more likely to keep their curtains and blinds open at night.

Evaluations of programs taking such actions have previously shown success in significantly lowering the incidence of crime [11, 42].

2.2. Operationalizing Natural Surveillance

In this section, we will review previous research into natural surveillance with the aim of finding how it has been operationalized in the past. With this knowledge we select relevant features to be included in our scalable methodology. Furthermore it provides us with previous findings on the subject, which we can use to put our results in context.

¹<https://www.securedbydesign.com/>

²<https://www.politiekeurmerk.nl/>

2.2.1. Manual Approaches

Research into CPTED and thereby natural surveillance has mainly been driven by manually collecting data through surveys and observation studies, both in person and virtual. This section will highlight some of the recent works taking such an approach.

- In 2009, Reynald [42] created a observational instrument to measure guardianship, the ability of individuals to prevent the occurrence of crime, and relate it to the CPTED characteristics of territoriality, milieu and image and natural surveillance. Guardianship was quantified by observers on a four level scale:
 1. **Invisible:** "no evidence that the property is occupied";
 2. **Available:** "evidence that the property is occupied";
 3. **Capable:** "whether the occupant(s) monitored observers or carried out general surveillance of their property and street";
 4. **Intervening:** "whether occupants physically intervened during the course of observations, by approaching observers with questions or comments regarding the purpose of their presence on the street".

Surveillance was measured on a 5 point scale by observing the extent to which the view of the property windows from public space was obstructed by physical features such as trees and walls. As can be seen in Figure 2.1, results showed a significant positive correlation between guardianship and surveillance opportunities, meaning that as surveillance increased, residents were more likely to show intervening behavior.

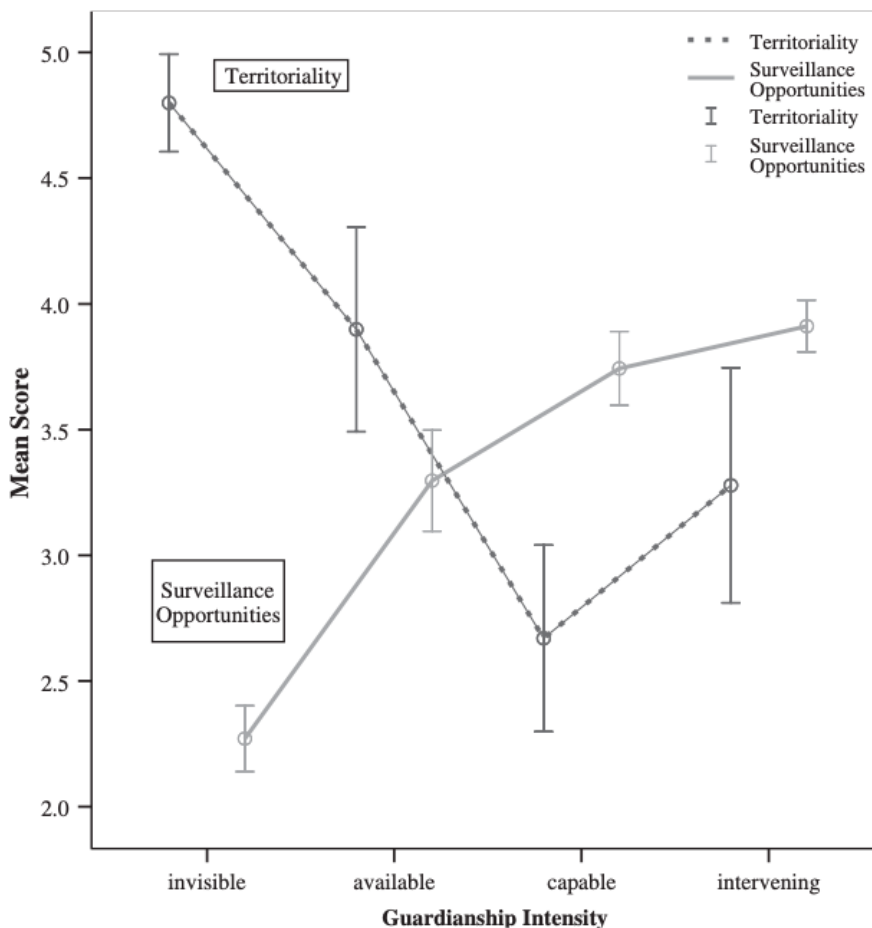


Figure 2.1: Results of [42] showing the correlations between guardianship, surveillance and territoriality.

- A 2017 study by Peeters et al. [40] performed observations of 1551 houses in the city of Ghent. Using their own observational instrument that took house, street and neighborhood characteristics into account, they tried to capture multiple CPTED characteristics including natural surveillance. At property level surveillance was measured by a simple binary variable stating if the property had either "no visibility" or "clear visibility" to neighbors. To assign a score for surveillance at street level, this data was aggregated and the percentage of houses with good visibility to neighbors was used. The paper concluded that houses that are not visible to their neighboring houses are linked to a higher risk of burglary, except for houses in the city center, where surveillance did not show any significant influence.
- A 2017 study by Lee, Jung, Lee, and Macdonald [29] developed a model for street crime prediction based on physical characteristics of the streetscape in a low-rising housing area in South Korea. As a unit of analysis, observation points along the street were chosen and data was collected on characteristics within the field of view of each observation point. For this specific neighborhood, a 20 meters radius around each observation point was chosen. This is visualized in Figure 2.2

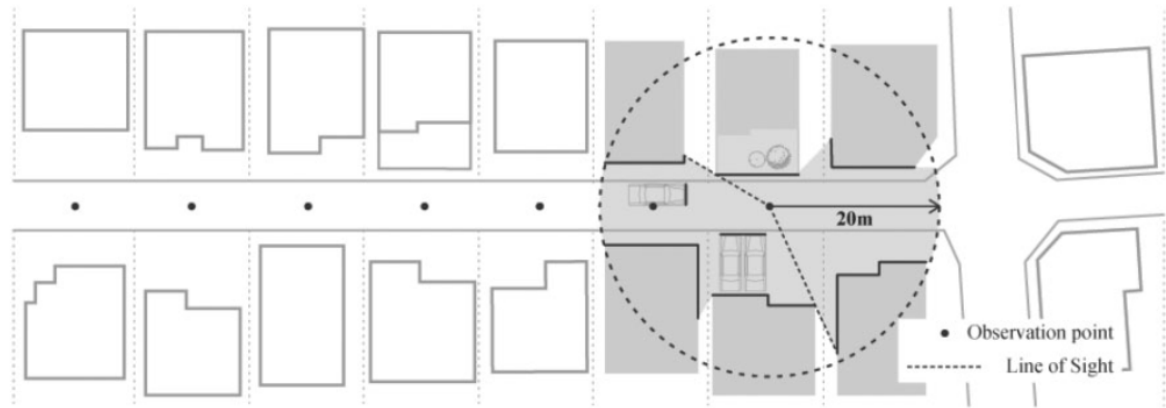


Figure 2.2: Visualization of the unit of analysis of the 2017 study by Lee, Jung, Lee, and Macdonald [29]

Data on a total of 18 variables were collected of which 14 were related to natural surveillance. These were based on a literature study combined with some variables that were specific to the properties within the studied area. All variables were manually collected through an observation study. Out of the 14 variables related to natural surveillance 10 showed to be significantly correlated with the occurrence of theft and were included in the model. These included:

- The number of balconies and verandas.
- The number of visual obstructions.
- Visibility from windows facing the street.

How exactly the value for visibility from the windows was determined is not clarified in the paper.

2.2.2. Computational Approaches

More recently, computational approaches on quantifying safety have been developed, of which some also include some measure of natural surveillance. This section will provide an overview of these related works.

- In 2015 Shach-Pinsky and Ganor [47] developed a security index based on a literature review with the goal of identifying unsafe areas by analyzing urban morphology.

In a 2019 study by Shach-Pinsky [46] this index was further developed and applied to Tel-Aviv (Israel) and Portland (United States). Two sets of security maps were created: one for daytime and one for nighttime security. The main ambition of the research was to develop a generic model that could objectively measure the level of security of areas in every city, only relying on urban morphology parameters. A literature review yielded 35 elements as having the most influence on the sense of security in the built environment. These were split into three different categories:

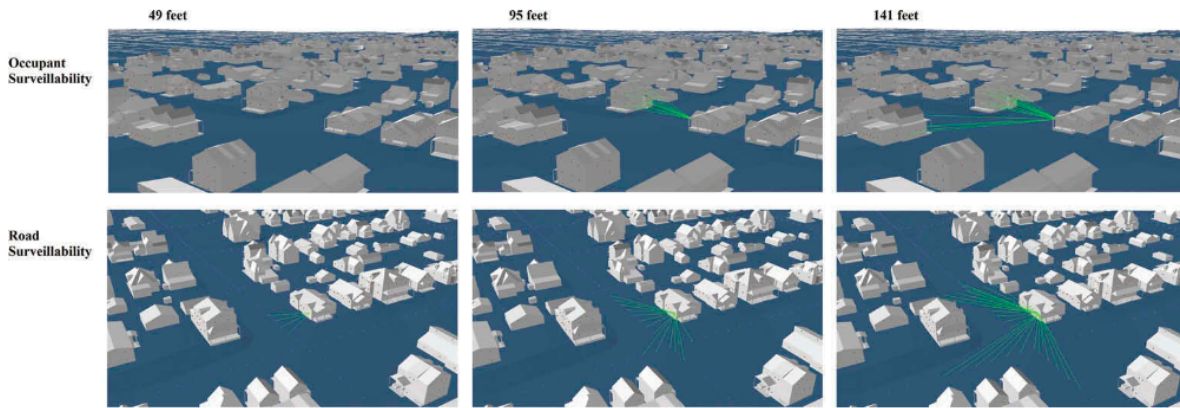


Figure 2.3: Example of the output for both road surveillability and occupant surveillability generated by the 2020 Amiri study [1].

1. **Detailed urban elements:** these were elements that were judged to have an important role on the security of areas but could not be measured comparatively in every urban environment due to a lack of data on these elements. These included: CCTV, gates and fences, building entry locations and windows (the latter two being a limitation which this work will try to resolve).
2. **Supportive aspects:** this group contained variables that influence security but are difficult to quantify. These included whether or not spaces are actively being used, the way spaces are being maintained and the quality of the justice system.
3. **Measurable urban elements:** these were the urban elements that influenced the sense of security for which there was data available to quantify them in the urban environment. These were: (1) mixed uses (2) street light density (3) building proximity and (4) number of intersections and (5) distance between junctions.

Each of the included features were given a score between 1 (most secured) and 5 (least secured). For each of these elements a raster map was created within the ESRI ArcMap software, which were integrated into one weighted-layer raster map summing up all five layers. Results showed that the model could predict and identify small hotspots where crime events may occur.

- A 2020 study by Amiri and Crain [1] proposed a natural surveillance model in three dimensions. They used a combination of Pictometry oblique aerial imagery (captured by low-flying planes) and field observations to create 2D and 3D models of the studied area. The selected area contained 324 parcels within the medium-sized US city of Spokane. The models generated from the imagery and observations contained information on the location of buildings, building openings (i.e. doors and windows represented as point features), territorial barriers and vegetation. Collecting and georeferencing the spatial data for these models took approximately 1 year to complete.

After the models were created, an analysis was performed using the ESRI ModelBuilder software to measure two aspects of natural surveillance:

- **Road surveillability:** the surveillability of building openings from the streets. It was quantified by counting the number of unobstructed sightlines from building openings to points placed on road centerlines.
- **Occupant surveillability:** the surveillability of building openings as seen by neighbouring building openings. This study quantified occupant surveillability by counting the number of unobstructed sightlines between building openings.

The lines of sight used to quantify these two aspects were calculated with different maximum distances derived from eye-witness identification literature. An example of the output of this whole process can be seen in 2.3.

Alongside this, the study investigated which architectural and landscape features had the most impact on visibility. The study showed that the presence and placement of street trees did not impact

surveillability. Furthermore, yard vegetation was shown to have the largest effect on reducing occupant surveillability and territorial barriers had the largest effect on reducing road surveillability.

3

Methodology

This chapter will provide a detailed explanation of, and reasoning behind the chosen methodology. It will discuss the included features and the data pipeline used to extract these features, along with the datasources used as input for this pipeline.

3.1. Selected Features

To capture the notion of natural surveillance in numbers, first a selection must be made on which features to use. The features chosen to be extracted from urban data closely resemble the features in the previous works by Amari and Crain [1] and Peeters et al. [40] described in more detail in the previous chapter. The features are revolved around sightlines between two fixed points in space used to quantify two aspects of natural surveillance, road surveillability and occupant surveillability:

- **Road surveillability** is the surveillability of building openings from the streets and vice versa. We will measure this by counting the number of building openings that have an unobstructed sightline to a given point sampled along the road network.
- **Occupant surveillability** is the surveillability of building openings by other neighboring building openings. To measure this we will count, for each building opening, the number of other building openings that should have an unobstructed sightline to it.

These features were selected because they are (1) objectively measurable, (2) are an established way to measure natural surveillance [1, 7, 35, 37, 40] and (3) are relatively insensitive for temporal differences in the data they are computed from, since building openings are static elements in the urban layout. To calculate these features, two things are needed for the entire urban area to analyze: (1) the road network and (2) the location of building openings. While data on road networks is widely available from various data sources, this is definitely not the case for the location of building openings [46, 47]. This poses a challenge for computing these features on a large scale. In the next part of this chapter, the data pipeline and data sources for obtaining this data and computing the selected features from them will be discussed.

3.2. Data Pipeline

To obtain data on the road network and building opening locations needed to compute the selected features at scale, a data pipeline is constructed. The pipeline consists of various data sources and processing steps. In this section, the whole pipeline will be explained in detail.

3.2.1. Data Collection

As a first step in the pipeline, data from both OpenStreetMap and Google Street View is collected. An overview of the whole data collection process can be seen in Figure 3.1. The goal of the process is to obtain three sources of information which can later in the pipeline be combined to obtain data on opening locations and possible sightlines throughout the urban area of interest. These are: (1) the area's street network, (2) the building footprints (i.e the outlines of a building's exterior walls as seen from above) of all buildings within the

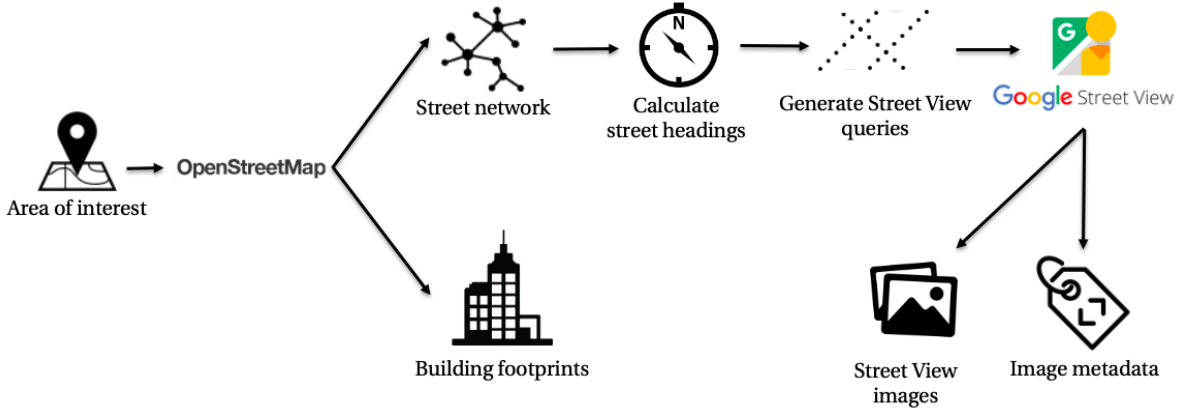


Figure 3.1: Overview of the data collection process.

area, and (3) street view imagery of building facades within the area along with the included metadata.

Obtaining the Street Network and Building Footprints

To start of the data collection process, we obtain the street network and building footprints for the area of interest. Data on the street network is used for creating sample points along the network, for each of which data will be collected. The building footprints have two use cases in the pipeline, which are:

1. Acting as a source of a-priori knowledge on the possible location of building openings, since most building openings are located along the exterior walls of buildings.
2. Providing data on which buildings block certain sightlines onto the street and other building openings. Including the location of trees was also considered for this purpose, since these are also well indexed throughout various cities. However, previous research indicated that, contrary to architectural features, trees had a negligible impact on visibility [1] and thus the choice was made to not include such data in the pipeline.

Both the street network and building footprints can be obtained from OpenStreetMap¹: a free-to-use open-source project for creating and distributing worldwide geographic data. For accessing the OpenStreetMap data we use OSMnx [5]. OSMnx is a third-party Python library which can be used to automatically download street networks and building footprints, and makes them available as convenient data structures to use later on in the pipeline. The area to download can be restricted by providing either a polygon with the coordinates of the area of interest or an address and distance from that address. An example of the resulting street network and building footprints for a neighborhood in Amsterdam can be found in Figure 3.2.

Obtaining Street Level Imagery of Building Facades

We use street level imagery of building facades as a data source for locating building openings throughout the urban area. Previous manually conducted research on the topic, which used Google Street View as a Systematic Social Observation (SSO) tool to retrieve this data, has shown this being a viable datasource for doing so [28].

As a source for these images, both **Mapillary** and **Google Street View** were considered. While the Mapillary platform makes its images available free of charge, a significant portion of its images are captured through the front windows of cars and are thus in the direction of traffic flow. In contrast, Google Street View features full 360 degree panoramic images by default. Since we are interested in imagery of the building facades, which are largely located orthogonal to the streets, the Google Street View data fits our use-case better. Furthermore, the coverage of Mapillary data is very dependent on the area, and often does not cover streets which have less traffic passing through them, such as streets heading into residential areas. These, however, are also areas of interest for this research and Google Street View has better coverage for these areas specifically. For these two reasons, Google Street View was used as datasource for the street view imagery.

¹<https://wiki.openstreetmap.org/>

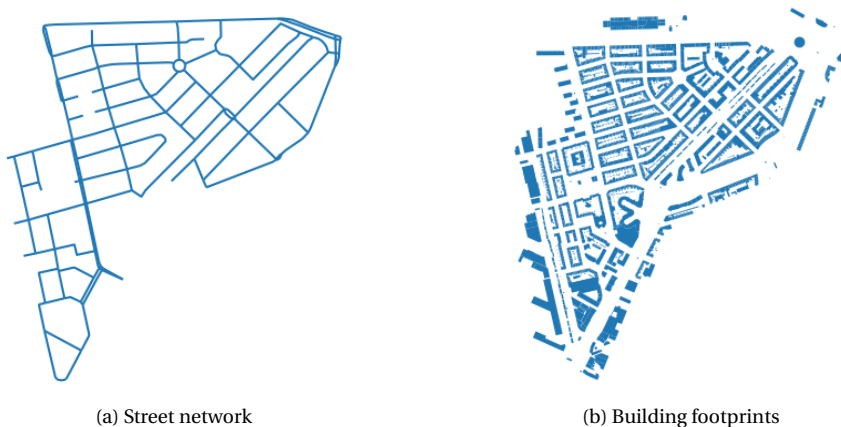


Figure 3.2: Street network and building footprints of the Staatsliedenbuurt in Amsterdam

We use the Google Street View Static API to obtain the imagery. To request an image from the API, the following parameters need to be provided:

- **Location:** latitude and longitude of the location to request an image for. The API will search and return the closest Street View image within a 50 meter radius around the provided coordinates.
 - **Heading:** a number between 0 and 360 indicating the compass heading of the camera, i.e. relative to compass north.
 - **Pitch:** Similar to heading, but in the vertical direction.
 - **Field of view:** a number between 0 and 120 indicating the portion of the panorama to be displayed. This parameter has a maximum allowed value of 120, meaning that a maximum of one third of the panoramic image can be requested at once. When using a fixed size image, this parameter in essence represents zoom, with a smaller fields of view representing a higher level of zoom.
 - **Size:** The output size of the image. A maximum of 640 x 640 pixels is allowed.
 - **Source:** Since the Google Street View platform also includes indoor images, this parameter can be used to exclude those, and only use the images captured outdoors.

While we can use fixed values for the *pitch*, *field of view*, *size* and *source* parameters, the location and heading parameters differ per image. These two variables are computed from the street network previously obtained. Since we are interested in building facades, which are mainly orthogonal to the street network, we want the heading parameter to be defined relative to the heading of the streets. To do this, first the heading of each street segment in the network relative to compass north is computed. The desired headings for both the right and left side of the street are then obtained by adding 90 and 270 degrees to the street heading.

We then sample the street network along regular intervals (10m) to obtain the latitude and longitude parameters. The sampled locations are then matched with the heading of the corresponding sections of the street to create the requests for the API. A visualization of this process can be seen in Figure 3.3.

Since Google only charges for the request of the actual image, and not for requesting the corresponding metadata, we first request metadata for each of the sampled locations. This metadata contains information about the availability of street view imagery for the provided location, and if imagery is available, the actual location where the image was captured. This location usually differs several meters from the location included in the request to the API. Duplicates are removed from the returned metadata to prevent requesting the same image more than once, thus preventing unnecessary API charges. The corresponding images for the remaining metadata are then requested from the API at a cost of \$7 per 1000 images at the time of writing. Examples of the returned images can be seen in Figure 3.4.

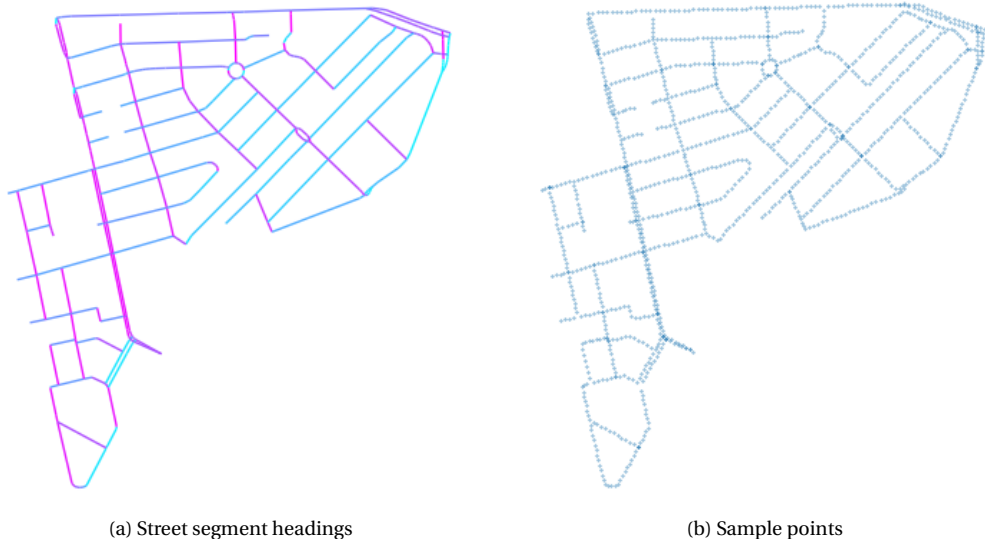


Figure 3.3: Visualization of the heading of the street segments relative to compass north and sample points along the street network. These two are combined to generate the requests for the Google Street View Static API.

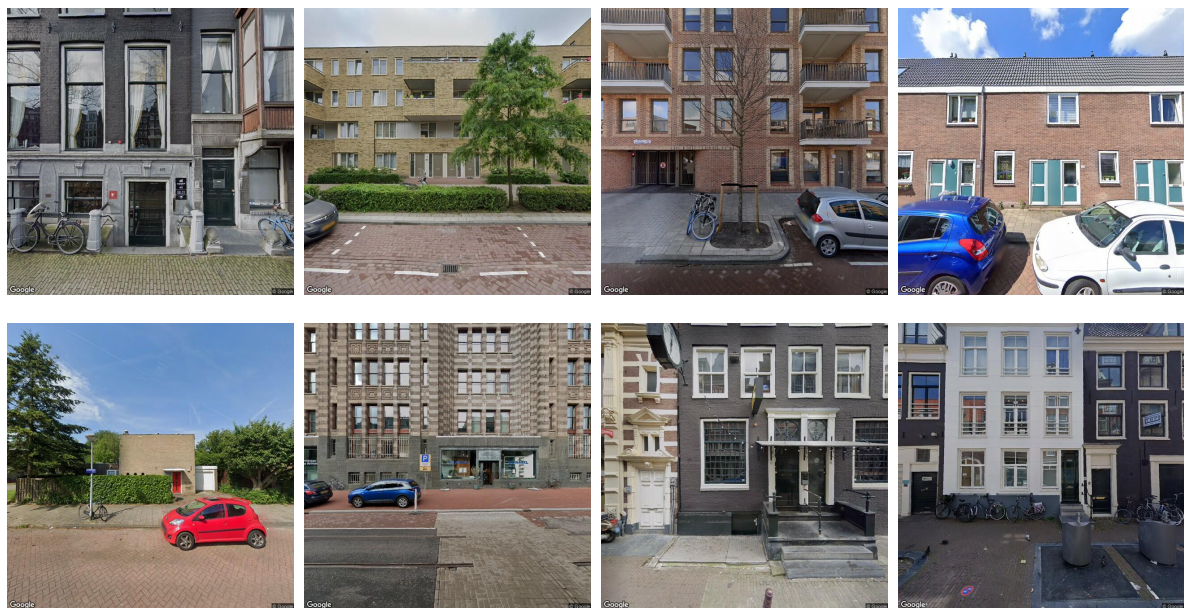


Figure 3.4: Examples of street view imagery collected from the Google Street View Static API throughout various neighborhoods in Amsterdam.

3.2.2. Data Processing

With the street network, building footprints and street view imagery now collected, the data is ready to be processed. By combining this data, it is possible to compute the geolocation of the building openings and, from them, the sightlines as described in Section 3.1. First, we obtain the estimated locations of building openings for the entire area of interest. An overview of this process can be seen in Figure 3.5. This process can roughly be divided into two steps: (1) detecting the building openings within the street view imagery and (2) geolocalization of the detected building openings.

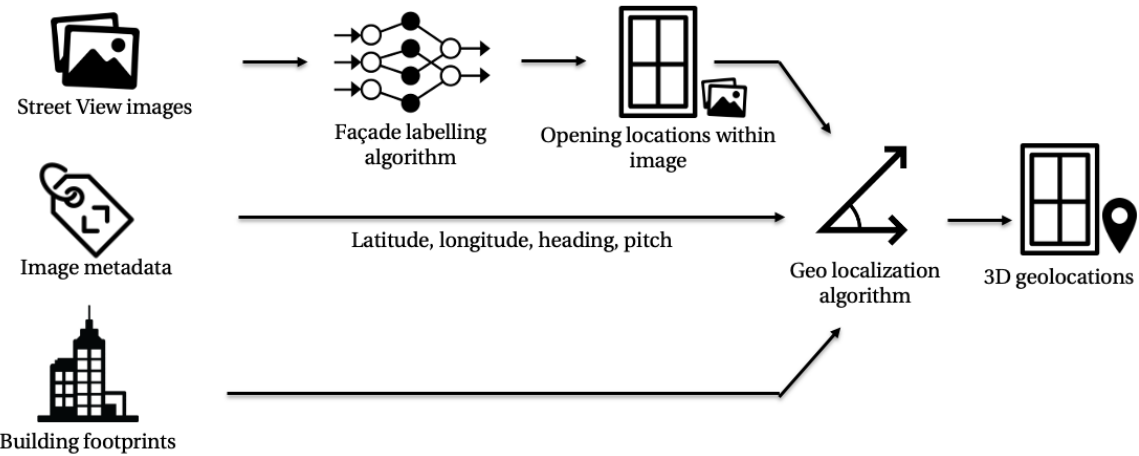


Figure 3.5: Overview of the processing steps used to obtain the geolocations of building openings throughout the area of interest.

Detection of building openings within street view imagery

As a first step in obtaining the locations of building openings throughout the city, we detect the presence of building openings within the street view imagery previously collected. To do this, we use the facade labeling algorithm developed by Li et al. [30]. This algorithm detects keypoints of windows within the image using 2D heatmaps. It then links sets of four keypoints (top-left, bottom-left, bottom-right, and top-right) together using an end-to-end network which has been trained on labeled images with varying facade structures, viewing angles, lighting and occlusion conditions.



Figure 3.6: Output of the facade labeling algorithm by Li et al. [30] on street view imagery collected throughout Amsterdam.

We feed the street view imagery through the facade labeling algorithm to obtain the pixel locations of the four keypoints for each detected opening within the image. An example of the returned output for several images can be seen in Figure 3.6. These keypoint will be used as input for the geolocalization algorithm described in the next section.

Geolocalization of building openings

Next, we compute the estimated geolocation of each detected building openings in the street view imagery. This is done by combining the location of the opening within the image with that image's metadata (latitude, longitude and heading) and the building footprints as detailed in Section 3.2.1.

We use the geolocalization algorithm developed by Qiu et al. [41] including the modifications introduced in [48]. The geolocalization of the building openings proceeds as follows:

1. From the metadata of each street view image, the latitude and longitude of the Google Street View camera at the time the image was captured, l_c , is extracted. The heading, $\theta_{heading}$, and *field of view* parameters are not contained in the metadata but are stored at the time the image is requested.
2. By combining the *field of view* parameter with the pixel location of a building opening keypoint, the angle β , relative to the heading can be calculated. $\theta_{heading}$ and β then give us the estimated direction of the keypoint relative to compass north, as is visualized in Figure 3.7a.
3. A 50 meter long ray, r , is cast from the Google Street View camera location in the estimated direction of the building opening.
4. From the set of building footprints previously collected, which we'll call B , all building footprints within radius of the ray are selected into a set B_c . Then, intersections of the ray with all building segments $b \in B_c$, are computed.
5. From all intersections i_s of the ray with the building segments, the distance to from the Google Street View camera to the intersection, d_{cs} is recorded. The intersection which smallest d_{cs} , then gives us the building segment \hat{s} containing the building opening and i_s is then selected as the estimated latitude and longitude position of the building opening keypoint.
6. Given the distance d_{cs} of i_s , an estimated altitude of the keypoint can be determined by using the vertical location of the keypoint within the image (similarly to step 2, but in the vertical direction), estimated height of the Google Street View camera ($\pm 2.5\text{m}$ according to online documentation²) and basic trigonometry.

This process provides us with the latitude, longitude and altitude of all four keypoints for each of the building openings detected in the street view imagery. From these 4 keypoints we compute its center-point and store it as the building opening's location. A visualization of the output of this process can be seen in Figure 3.8.

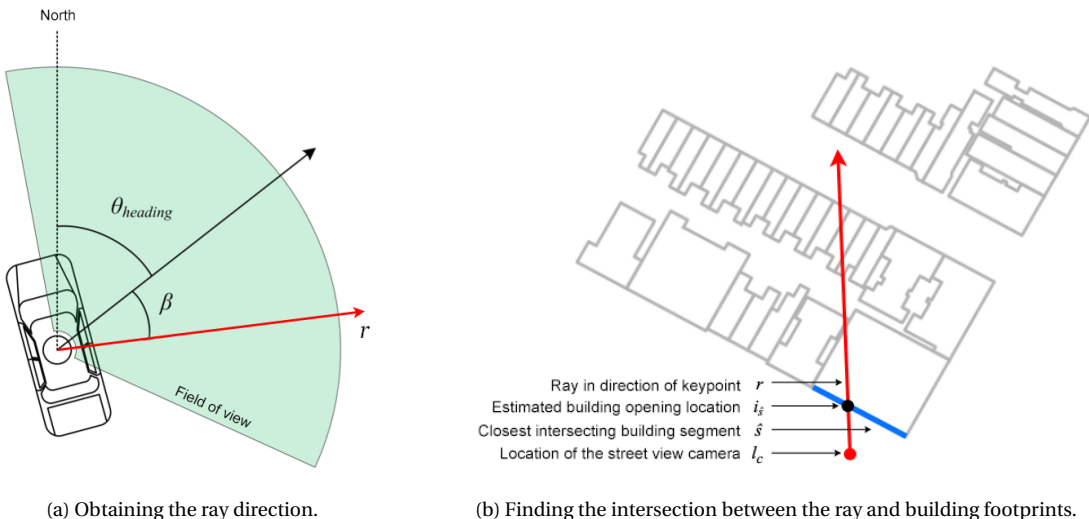


Figure 3.7: Visualization of the geolocalization process. Figures adapted from [41] and [48].

²A Glimpse of Google's Fleet of Camera-Equipped Street View Cars: <https://petapixel.com/2012/10/15/a-glimpse-of-googles-fleet-of-camera-equipped-street-view-cars/>



Figure 3.8: 3D visualization of the output of the geolocalization algorithm for building openings in the Staatsliedenbuurt, Amsterdam. Each white dot represents the center of a building opening.

3.2.3. Calculating Road Surveillability and Occupant Surveillability

With the latitude, longitude and altitude of the building openings now estimated, we can proceed with the calculation of the features, representing road surveillability and occupant surveillability. As described in more detail in Section 3.1, these features are revolved around sightlines between two fixed points in space. These two points are:

1. A sample point along the road network (the Google Street View camera location) and a building opening, as a measure of road surveillability.
2. A building opening and a neighboring building opening as a measure of occupant surveillability.

Furthermore, we constrain the sightlines that are included in these features on three properties:

1. **Building opening altitude:** As previous research indicated that vision from ground floor windows has a greater diminishing effect on street crime than the higher floor level windows [29], we exclude all sightlines to and from openings of which their center-points are above certain altitude, representing a floor level (1st floor, 2nd floor, etc.). We will further refer to this altitude as a_{max} .
2. **Sightline length:** On the basis of a review on eye-witness literature [18, 23, 31, 33, 36] as performed in [1], we exclude sightlines that have a length greater than a certain amount of meters, which we will further refer to as d_{max} .
3. **Field of view:** We define an angle θ_{fov} as the field of view observable from an opening. All sightlines that fall outside this field of view are excluded.

The obtained results are then aggregated to the scale of streets and neighborhoods for further analysis. The remainder of this section will go into the specifics of calculating these features.

Road Surveillability

For computing the sightlines used as a measure of road surveillability, we make use of the fact that the vantage point the Street View data was captured from is the road itself. Therefore we can count each building opening detected within the image, which has an altitude lower than a_{max} , and a distance lower than d_{max} as a sightline from the geolocation of the building opening to the location of the Street View camera. This will give us the number of unobstructed sightlines from building openings to the points sampled across the road network. A visualization of this can be seen in Figure 3.9.

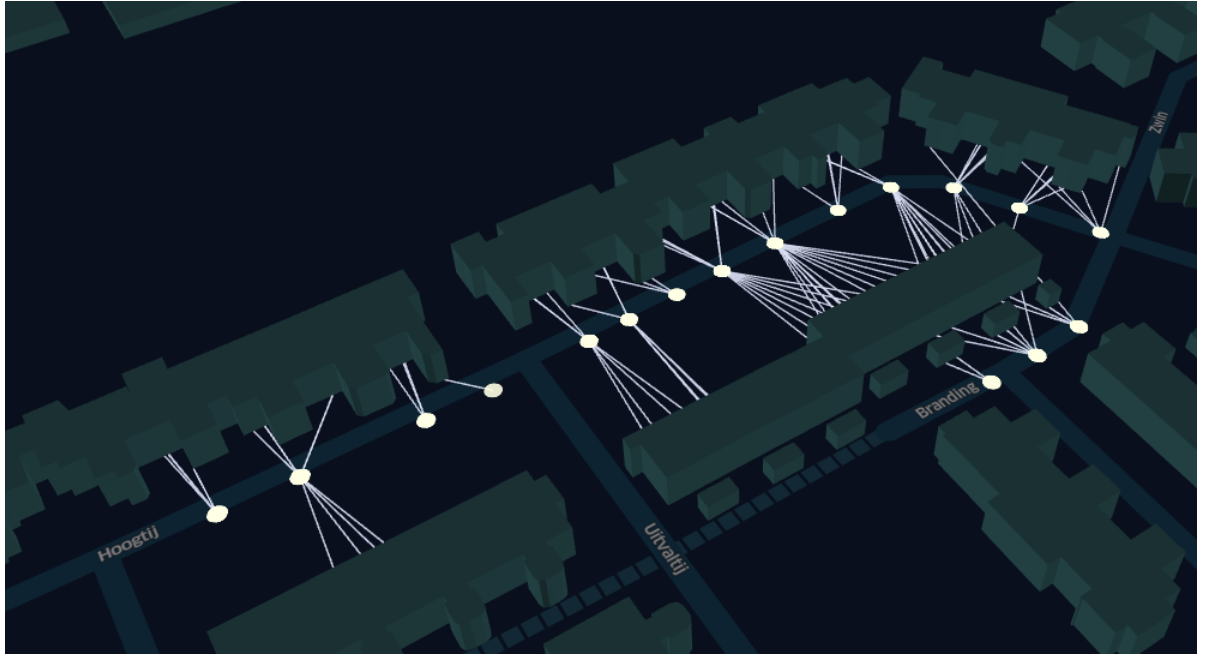


Figure 3.9: Visualization of the computed sightlines from the street to the building openings as used as a measure of road surveillability.

Occupant Surveillability

To compute our measure for occupant surveillability, we compute, for each building opening, the number of building openings that should have an unobstructed sightline to it. This is done in the following steps:

1. We project all location information from the World Geodetic System to a local coordinate reference system, e.g. epsg:28992 for the Netherlands. Furthermore, we create a R-tree [19], a spacial index, for the building footprints. This way we can efficiently query the building footprints based on location.
2. For a given detected building opening $o_{viewpoint}$ with an altitude lower than a_{max} , we select all neighboring building openings that have an altitude lower than a_{max} and are a maximum of d_{max} meters away from $o_{viewpoint}$ into a set $O_{neighboring}$.
3. We construct all sightlines from $o_{viewpoint}$ to all openings $o_{neighbor} \in O_{neighboring}$. We call this set of sightlines S .
4. For each sightline $s \in S$ we obtain the set of building footprints B which could possibly block the sightline by querying the R-tree. We then check if s intersects a building footprint in B . If such an intersection exists, we consider s blocked and remove it from S .
5. For all remaining sightlines $s \in S$, we calculate the angle θ_s between s and the normal vector of the building segment containing $o_{viewpoint}$ (see \hat{s} in Figure 3.7b). If $\theta_s > \frac{1}{2}\theta_{fov}$, we deem s outside the field of view of the building opening and remove it from S . See Figure 3.10 for an visualization of remaining sightlines in S after this step. Note that due to the restriction on sightline angle, a sightline from $o_{viewpoint}$ to $o_{neighbor}$ does not imply that a sightline from $o_{neighbor}$ to $o_{viewpoint}$ also exists.
6. For all s left in S , we take the corresponding $o_{neighbor}$ and add 1 to its sightline count, $o_{\#sightlines}$.

Steps 2 to 6 are repeated for each detected building opening. This results in a score for each building opening representing by how many other openings it could be observed.

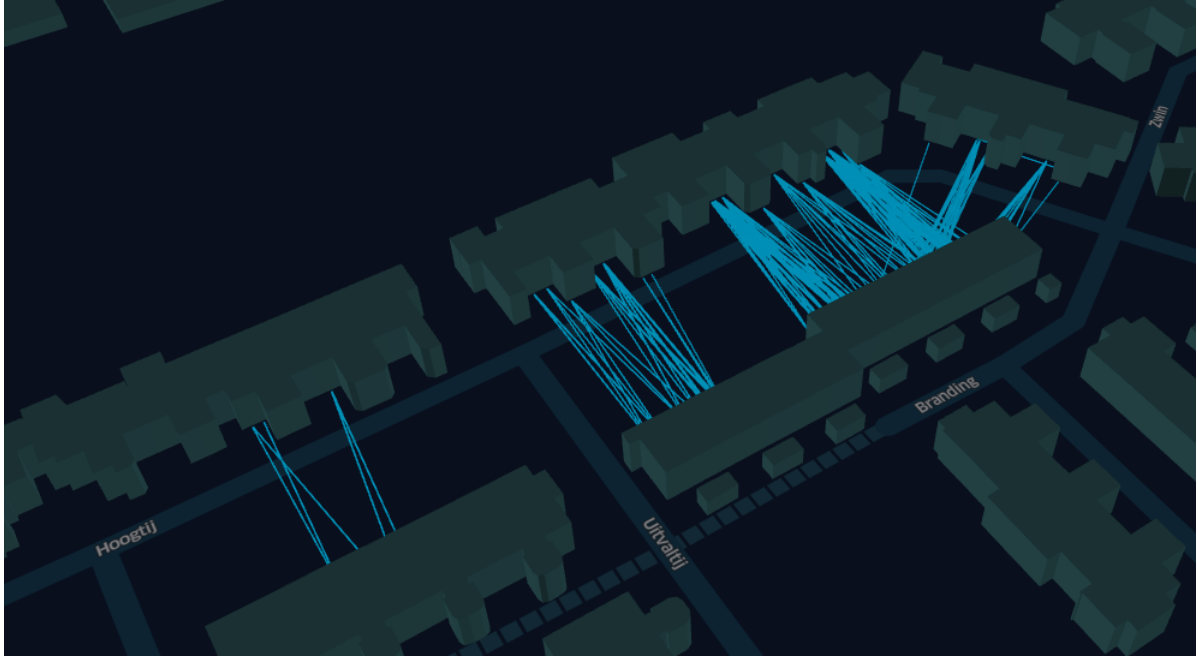


Figure 3.10: Visualization of the computed sightlines from building opening to building opening as used as a measure of occupant surveillability.

Data Aggregation

Our calculation of road surveillability and occupant surveillability, described above, results in two sets of points with are assigned a score representing how well they can be observed. A set of points along the road network for road surveillability, which we'll call R , and a set of building openings for occupant surveillability, which we'll call O . To aggregate these feature values to the level of streets and neighborhoods for further

analysis we link the points in R and O to a specific street segment t . Here, a street segment is defined as a section of the street between two junctions, or between a junction and the end of the street, if the street has a dead end.

We link the points to a the street segment by working our way back to the sample points along the road network that resulted in the creation of the data (see Section 3.2.1 and Figure 3.3). A building opening is thus linked to the Street View image in which it was detected, which in turn is linked back to the street segment that was sampled to request that image. The points along the road network are linked to a street segment in a similar manner.

With the points in R and O linked to a street segment t , we calculate the following two features, normalized for the street segment's length:

$$\text{Occupant sightlines per meter}_t = \frac{1}{t_{length}} \sum_{o \in O_t} o_{\#sightlines}$$

$$\text{Road sightlines per meter}_t = \frac{1}{t_{length}} \sum_{r \in R_t} r_{\#sightlines}$$

Where O_t and R_t are the points in O and R linked to street segment t , t_{length} is the length of street segment t in meters and $o_{\#sightlines}$ and $r_{\#sightlines}$ are the number of sightlines observing points o and r . A visualization for the road sightlines per meter feature for each street segment can be seen in Figure 3.11.

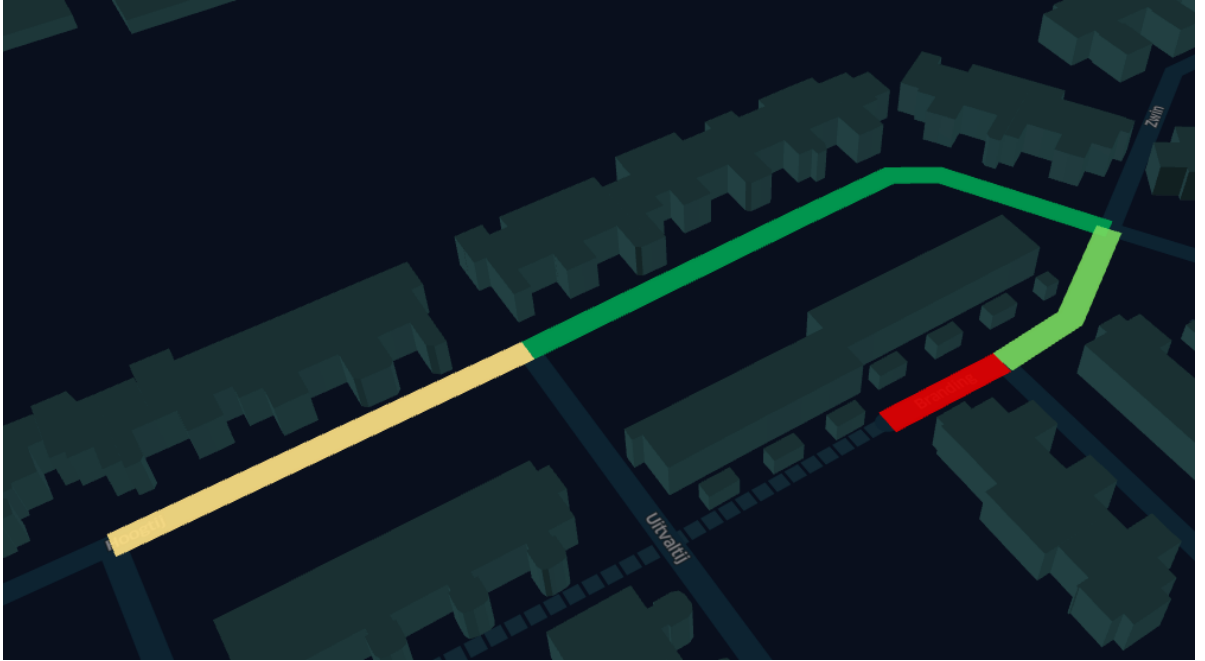


Figure 3.11: Visualization of the road sightlines per meter feature after the aggregation step. Red is lower, green is higher.

To calculate these features on the level of a neighborhood n , we sum the sightlines for all points belonging to the neighborhood, R_n and O_n , and divide this by the length of the sampled street network:

$$\text{Occupant sightlines per meter}_n = \frac{\sum_{o \in O_n} o_{\#sightlines}}{\sum_{t \in T_n} t_{length}}$$

$$\text{Road sightlines per meter}_n = \frac{\sum_{r \in R_n} r_{\#sightlines}}{\sum_{t \in T_n} t_{length}}$$

Here, T_n is the set of sampled street segments in neighborhood n . A visualization of the features aggregated to neighborhood level can be seen in Figure 3.12.

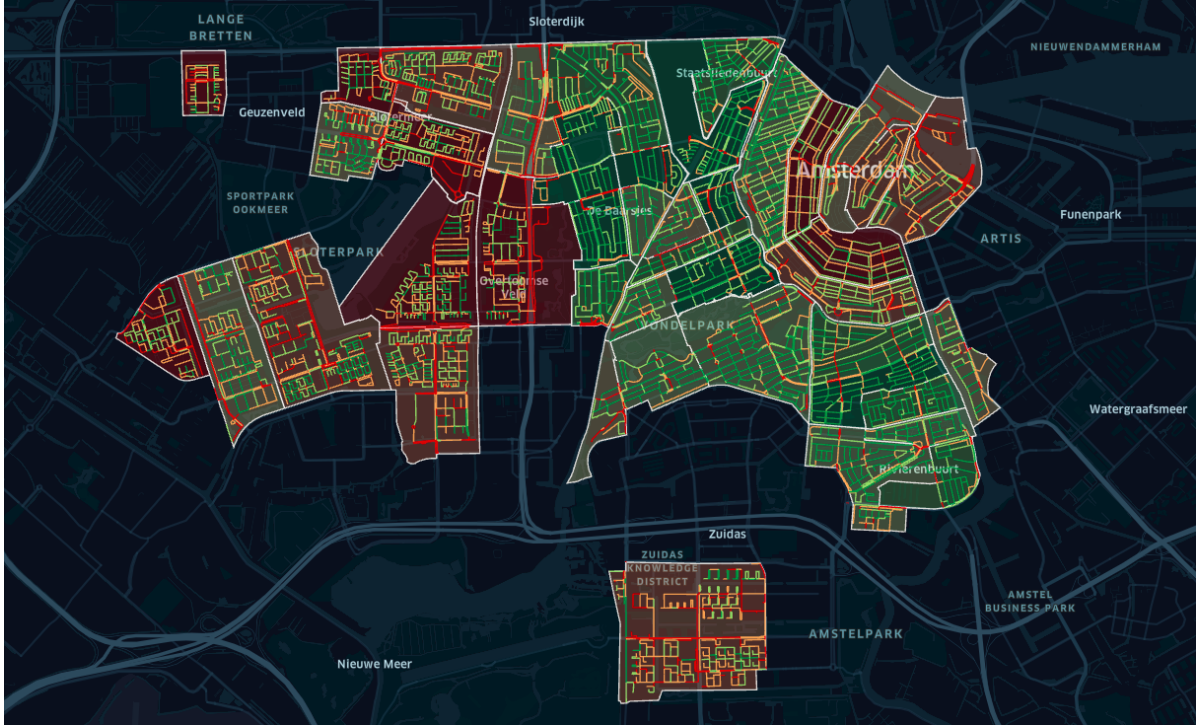


Figure 3.12: Visualization of the road surveillability feature for 43 neighborhoods in Amsterdam.

3.3. Evaluation

To evaluate the performance of our described methodology, this section will first provide a brief overview of the for this work relevant parts of previous evaluations of the used facade labeling algorithm [30] (described in Section 3.2.2) and geolocation algorithm [41] (described in Section 3.2.2).

Next, we create our own ground truth dataset consisting of 178 building openings belonging to 89 dwellings in the Dutch town of Noordwijk. We then apply our methodology to the same area and evaluate how well our method performs in estimating the geolocations of these building openings.

3.3.1. Previous Evaluations of Used Algorithms

Evaluation of the Facade Labeling Algorithm

The used facade labeling algorithm by Li et al. [30] was evaluated on several publicly available datasets and compared to seven other state of the art methods [8, 9, 17, 26, 27, 32, 53].

The datasets used to evaluate the model were: the Ecole Centrale Paris Facades (ECP) Database³, the eTRIMS dataset [25] and Graz50 dataset [45]. The ECP and Graz50 datasets contain more dense facades, with most images containing over 30 building openings. The eTRIMS dataset has more diversity in occlusion, light and distortion.

As an evaluation metric, pixel accuracy (the percentage of correctly classified pixels) was used. An comparison of the pixel accuracy of the different methods can be found in Table 3.1. As can bee seen, the algorithm by Li et al. [30] used in this work performs well on all three datasets with pixel accuracies of 84% on the eTRIMS dataset, 90% on the Graz50 dataset and 95% on the ECP dataset.

Evaluation of the Geolocalization Algorithm

The geolocation algorithm by Qiu et al. [41] was evaluated by letting a group of crowd workers annotate bounding boxes around trees in Google Street View imagery in New York and Amsterdam. The algorithm then estimated the geolocation of the trees from the bounding boxes provided by crowd workers. An annotation by a crowd worker was deemed to be correct if the estimated geolocation from the algorithm was within 5

³Ecole Centrale Paris Facades Database: <http://vision.mas.ecp.fr/Personnel/teboul/data.php>

Table 3.1: Comparison of performance of different state-of-art facade labeling algorithms, using pixel accuracy as evaluation metric.

	ECP	eTRIMS	Graz50
Gadde et al. [17]	72%	–	76%
Cohen et al. [8]	85%	71%	–
Kozinski et al. [27]	85%	–	82%
Wang et al. [53]	87%	–	–
Kozinski et al. [26]	87%	70%	84%
Cohen et al. [9]	87%	72%	85%
Liu et al. [32]	93%	91%	–
Li et al. (used) [30]	95%	84%	90%

meters of the corresponding tree in the ground truth dataset. Of these correct annotations the RMSE of the predicted geolocation was evaluated. The precision and RMSE were defined as follows:

$$P = \frac{\text{# of correct annotations}}{\text{# of all aggregated annotations}}$$

$$\text{RMSE} = \sqrt{\frac{\sum_{\text{correct annotations}} (\text{annotation error})^2}{\text{# of correct annotations}}}$$

Based on the quality of the provided annotations, the group of crowd workers was split into three equal-sized quality groups (low, medium and high). The annotations of a total of 99 workers (45 in Manhattan and 54 in Amsterdam) were deemed of good enough quality. The distribution of the resulting precision and RMSE for the 99 workers, split among the three different quality groups can be seen in Figure 3.13.

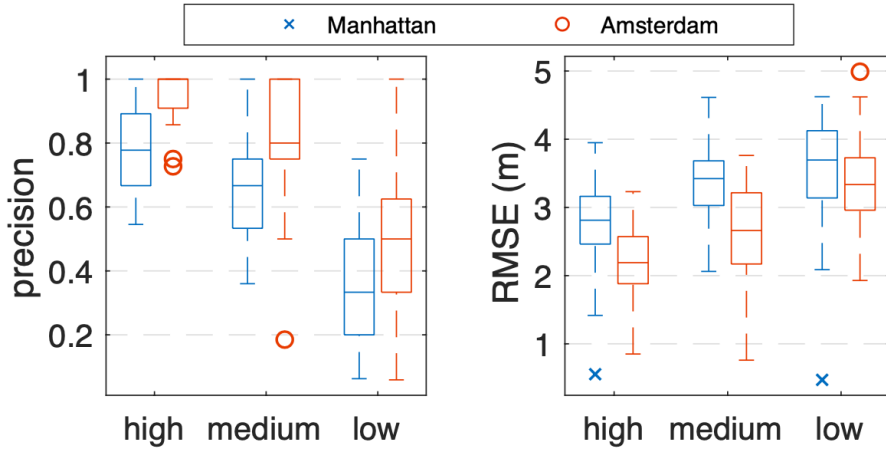


Figure 3.13: Precision and Root Mean Square Error (RMSE) for the geolocalization algorithm by Qiu et al. Figure adapted from [41].

As can be seen, for high quality workers the the median RMSE is less than 3 meters for both cities, with some task executions having a RMSE less than a meter. From this, it can be concluded that given high quality bounding boxes, such an error in localization is to be expected. However, note that in this evaluation on trees it was not possible to make use of a-priori knowledge of the tree's location. In this work, we make use of the building footprints to narrow down the possible positions of building openings, which is likely to result in smaller errors in the estimated geolocation, as will be demonstrated in the evaluation on our own dataset described in the next section.

3.3.2. Evaluation of Building Opening Geolocalization

Construction of a Ground Truth Dataset

To thoroughly evaluate the accuracy of the estimated building opening geolocations, a ground truth dataset containing such geolocations is needed. Since, to our knowledge, such a dataset does not publicly available, we constructed one from scratch. The steps that were taken to do so will be described below.

First, we obtained blueprints of four different types of terraced houses in the Dutch town of Noordwijk. A total of 89 dwellings in the area are built in one of these four styles. From these blueprints, the locations of the large windows along the facade were obtained. Since these drawings originate from before the buildings were built, minor inconsistencies with the actual buildings may exist (e.g. $\pm 15\text{cm}$). Furthermore, over the years, several buildings have undergone some form of renovation, such as the placement of dormers. Only the openings that were present in the blueprints in our possession were included in the dataset.

Next, the building footprints of these 89 dwellings were retrieved from OpenStreetMap. Please note that this geometry can contain positional inaccuracies of up to 30cm ⁴. This geometry is then split up into individual wall segments and the segments belonging to the street facades in the blueprints were manually selected. The measurements taken from the blueprints are then projected along these wall segments to obtain the latitude, longitude and altitude of 178 openings.

Evaluating the Accuracy of Estimated Geolocations

Subsequently, we ran our pipeline on the area containing the 89 dwellings. The openings detected in the Street View images were manually inspected. Out of the 178 openings, 34 were not visible in the obtained Street View data, of which 12 were blocked by bushes and/or trees and another 22 were either blocked by buildings or no street view imagery containing them was available. Examples of such images can be seen in Figure 3.14. This leaves 144 openings that our method could possibly have detected.



Figure 3.14: Examples of building openings that were not detected due to being blocked by trees or buildings

Out of these 144 openings, 120 were detected and geolocalized. A visualization of the ground truth and estimated geolocations can be seen in Figure 3.15.

The estimated geolocations of these 120 openings were than compared to the corresponding ground truth geolocations. First the longitudes and latitudes were projected to the local coordinate system epsg:28992, yielding an x and y coordinate in meters. As an error metric, the euclidean distance was used. The euclidean distance was calculated as follows:

$$d(t, e) = \sqrt{(t_x - e_x)^2 + (t_y - e_y)^2 + (t_{altitude} - e_{altitude})^2}$$

Where e is the estimated geolocation and t the ground truth geolocation of the centerpoint of the corresponding building opening.

⁴Positional accuracy of BAG data: <https://imbag.github.io/catalogus/hoofdstukken/gegevenskwaliteit#45-positionele-nauwkeurigheid>

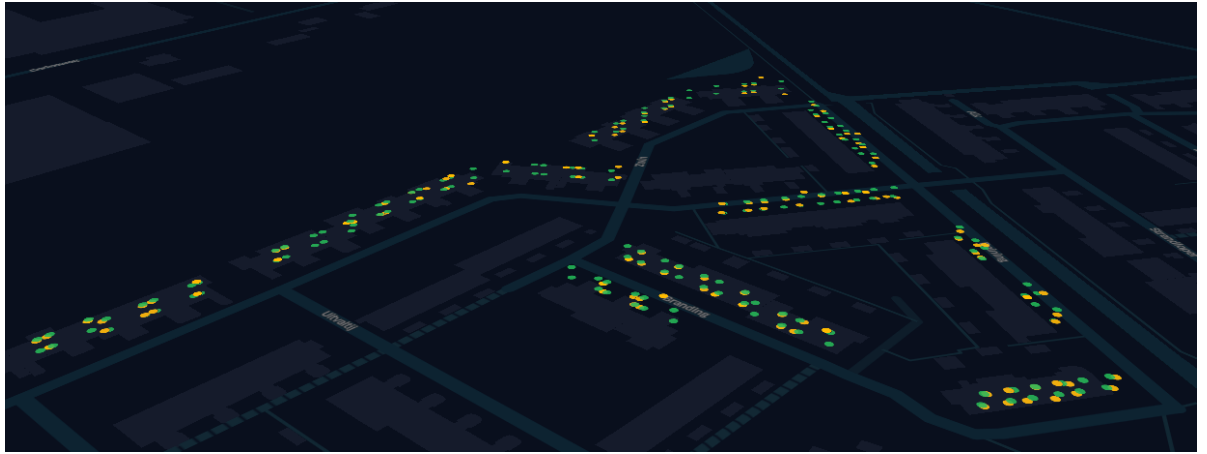


Figure 3.15: The ground truth geolocation (green), along with the estimated geolocation (yellow) of the 178 building openings used in the evaluation.

An overview of the results can be seen in Table 3.2 and Figure 3.16. Both algorithms seem to perform well in our method. The facade labeling algorithm detected **83.3%** of the visible openings. The geolocalization algorithm had mean error of **1.07 m** with a standard deviation of **1.09 m**, of which an error of $\pm 40\text{cm}$ could possibly be explained due to the way the dataset was constructed. The best prediction in our dataset had an error of only **4 cm**. The few large errors can occur due to the fact that the building opening is predicted to be on the wrong building segment. For example, the largest errors in our evaluation, were due to the fact that building openings were estimated to be on the wall of a shed, such as the one seen in middle of Figure 3.14, instead of the wall behind it. This, however, is not likely to be a common occurrence, since a lot of buildings have facades that have a straight exterior wall facing the street.

All things considered, we conclude that this evaluation has shown that this methodology is able to estimate the geolocations of building openings with a small enough error, that these can be used to provide an accurate estimate of natural surveillance.

Table 3.2: Evaluation results

Number of openings in dataset	178
Openings visible in imagery	144
<i>blocked by bushes/trees</i>	12
<i>blocked by building / no image available</i>	22
Recall (visible openings detected)	83.3% (120/144)
Mean Error in estimated geolocation	$1.08\text{m} \pm 1.09\text{m}$
<i>Minimum</i>	0.04m
<i>25th percentile</i>	0.57m
<i>50th percentile</i>	0.84m
<i>75th percentile</i>	1.17m
<i>Maximum</i>	7.99m

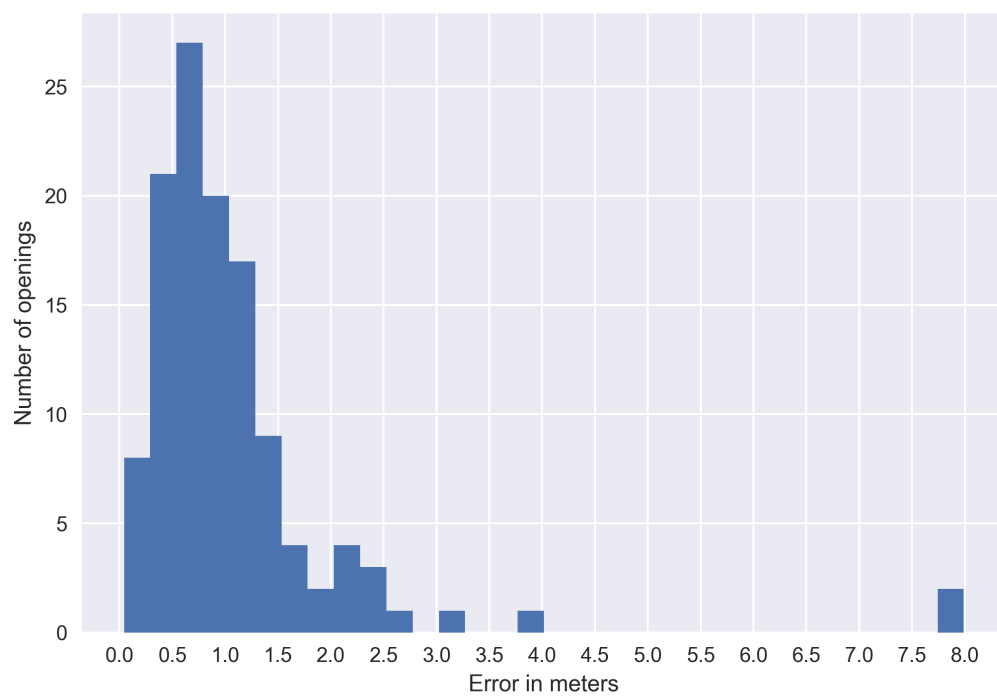


Figure 3.16: Histogram of the geolocalization errors.

4

Experiment Design

To answer **RQ2**: 'How do the measurements produced by the proposed methodology relate to the (perceived) safety of an urban area?', we conduct an experiment where we apply our methodology to a large set of neighborhoods throughout Amsterdam and correlate the results to a dataset on safety of these neighborhoods. Amsterdam is chosen because of it having a great variety of neighborhoods with different levels of reported safety. Furthermore, Amsterdam has an elaborate, well substantiated and publicly available dataset on safety: the Amsterdam Safety Index. This chapter will describe the used dataset and the conducted experiment in detail.

4.1. Amsterdam Safety Index

As our measure of (perceived) safety in an urban area, we make use of the Amsterdam Safety Index (in Dutch: Veiligheidsindex Amsterdam). This section will summarize the for our work relevant information on this index. All information in this section was retrieved from the index's justification document [2].

The Amsterdam Safety Index is an instrument used by the municipality of Amsterdam to track the main trends in the safety of the 104 neighborhoods that are under the jurisdiction of the Amsterdam police department. Besides Amsterdam itself, this also includes the cities of Aalsmeer, Amstelveen, Diemen, Ouder-Amstel en Uithoorn. A visualization of the neighborhood boundaries and their safety index scores can be found in Figure 4.1.¹ It has been in use since 2003 and its methodology was last revised in 2014. The methodology of the index has previously been described as well-considered and defensible by external reviewers [20].

In accordance to a proposal for safety indexes by the the Dutch Ministry of Justice and Security's knowledge centre, the WODC [52], the definition of safety used by this index is: *nuisance, feelings of unsafety and all forms of crime faced by citizens and businesses*. Safety is often divided into a subjective and an objective component. In this index the choice was made to not split safety up in two, but in three components: a **crime** component, a **nuisance** component and a **perceived safety** component. The choice to use a separate nuisance component was made to accommodate the special status nuisance has and the discussion if nuisance is a objective or subjective component. One of the main goals when developing this instrument was to be able to compare the safety of different neighborhoods at a certain point in time and track the developments on neighborhood safety throughout time, which makes it a useful tool to juxtapose our results with. The next sections will describe the datasources and technical details of the index.

4.1.1. Datasources

The index makes use of two datasources: police data and survey data. Where possible, both these sources are combined because on their own they both have their limitations regarding reliability. Police data suffers from under-reporting since not all crimes are reported to the police, and are thus not present in police databases. On the contrary, survey data suffers from over-reporting with a possible cause being the telescoping effect: crimes that fall outside of the surveyed period (e.g. a year) are reported to be more recent than they actu-

¹An interactive visualization of the Amsterdam Safety Index is available at: <https://data.amsterdam.nl/specials/dashboard/dashboard-veiligheid/d6006969-9d2a-413d-80a4-308932ed36f8/>

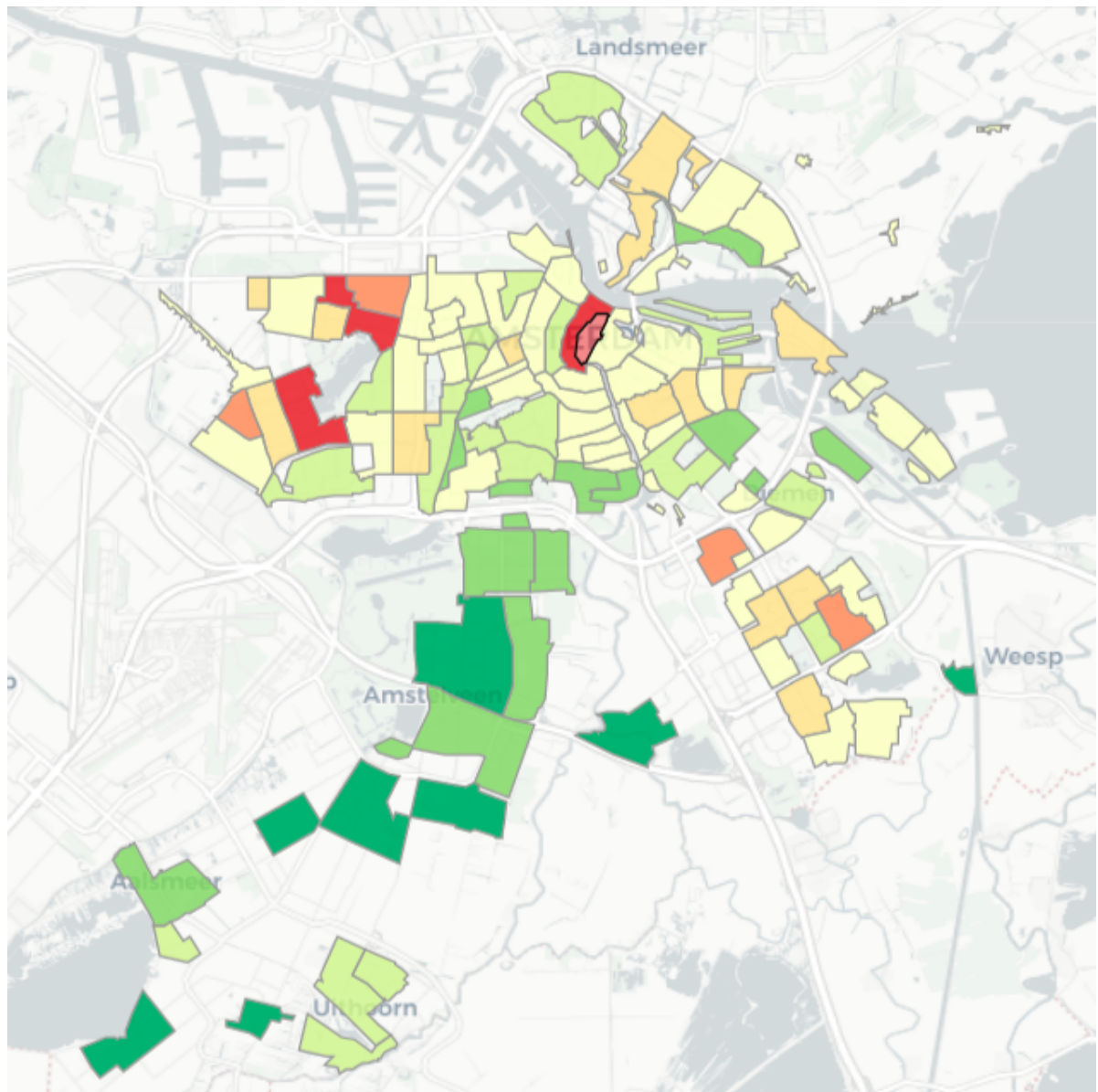


Figure 4.1: The 104 neighborhoods included in the Amsterdam Safety Index. Green is safer, red is unsafer.

ally are due to the impact the crime had on the victim [3]. By combining these sources where possible, the idea is these effects will be minimized. However, one of the criticisms of the index is that weights applied when combining these two datasources are somewhat arbitrary [3, 52]. As a counterargument to this, it is stated that altering these weights does not result in drastic changes in the rank order of the different neighborhoods.

4.1.2. Composition of the Index

As previously stated, the safety index is comprised of three subindices for **crime**, **nuisance** and **perceived safety**, which in turn are comprised of two or three elements. The main index is calculated by taking the average of these three subindices. The lower the index, the safer the neighborhood is. This section will describe the three main subindices and how they are calculated.

Crime Index

The crime index consists of police data and the victimhoods reported by residents in surveys. A distinction is made between High Impact Crime and High Volume Crime:

- **High Impact Crime (HIC)** are crimes that make a personal impact on the victim. Crimes that fall in this category are burglary and robbery into/from homes, street robbery, violence against people, criminal threatening, sex crimes and murder.
- **High Volume Crime (HVC)** are crimes that are commonly committed but have less of an impact on the victim. Crimes that fall in this category are burglary and theft into/from sheds, storage boxes, garages, businesses and vehicles, theft of all kinds of vehicles (cars, bikes, boats etc.), shoplifting and pickpocketing.

To calculate the HIC and HVC index for each neighborhood, the police and survey data are processed in several steps. These processing steps are largely similar to those of the nuisance and perceived safety index. We will show these steps for the crime index in detail to paint the picture. These steps are:

1. **Making the data comparable between neighborhoods:** For police data, this means that the incidence numbers for each crime are, dependent on the crime, divided by the number of residents, residences or businesses that are possible victims of the crime. For survey data this means removing outliers and dividing the number of victimhoods by the number of respondents per neighborhoods. This results in a *relative crime incidence* number (from police data) and *relative reported victimhood* number (from survey data) for each of the crimes that are part of the index.
2. **Indexing the data:** The relative crime incidence and victimhoods per neighborhood are indexed such that it becomes easier to see if incidence of a crime x is increasing or decreasing over the years. This is done by dividing by the average reported incidence in the 104 neighborhoods of base year 2014 and multiplying by 100:

$$\text{Crime incidence index}_x = \frac{\text{relative crime incidence for crime } x}{\text{average crime incidence for crime } x \text{ in 2014}} * 100$$

$$\text{Reported victimhood index}_x = \frac{\text{relative reported victimhood for crime } x}{\text{average reported victimhood for crime } x \text{ in 2014}} * 100$$

An index of 100 for a crime x thus means that the reported incidence of that crime is equal to that of an average neighborhood in Amsterdam in the year 2014.

3. **Merging police data and survey data:** For each crime, the reported victimhoods from the survey data and the crime incidence as indicated by police data is merged. This is done by applying weights to the two indices calculated in step 2. The police data gets a weight of $\frac{2}{3}$ and the victimhoods reported in the surveys get a weight of $\frac{1}{3}$. This is due to the notion that the police data gives a more objective view of crime incidence than the survey data:

$$\text{Crime specific index}_x = \frac{2}{3} * \text{Crime incidence index}_x + \frac{1}{3} * \text{Reported victimhood index}_x$$

4. **Combining indices of individual crimes into the HIC and HVC indices:** The individual indexes for each crime part of the HIC or HVC category are then averaged to calculate the HIC and HVC indices. One exception to this are the indices for murder and robbery, which count half. This is because these crimes are relatively uncommon compared to the other crimes. A small change in incidence of these crimes would otherwise have an unreasonably big impact on the index.
5. **Calculating the crime index:** The total crime index is then calculated by averaging the HVC and HIC indices.

$$\text{Crime index} = \frac{1}{2} \times \text{HIC index} + \frac{1}{2} \times \text{HVC index}$$

Nuisance Index

Nuisance as defined by the index is *all intended or unintended behavior directed against people, objects or goods that are not always punishable, but which are experienced as a nuisance and thus affect the social safety in a neighborhood*. Similarly to the crime index, the index is based on both police and survey data. The nuisance index consists of two subindices. These are nuisance by people and deterioration:

- **Nuisance by people** includes nuisance due to drug and alcohol related activities, noise, loitering and neighbors.
- **Deterioration** includes acts of vandalism, such as graffiti and damage to street furniture, as well as how well the neighborhood is maintained according to residents.

The subjective parts of the survey are converted to a scale from 0 to 100. The data is then processed in a similar fashion to the crime index, with the biggest difference being that the survey data has a weight of $\frac{2}{3}$ and the police data a weight of $\frac{1}{3}$, because it is estimated that nuisance is more often reported in surveys than to the police. The nuisance index is then calculated as follows:

$$\text{Nuisance index} = \frac{1}{2} \times \text{Nuisance by people index} + \frac{1}{2} \times \text{Deterioration index}$$

Perceived Safety Index

The last of the three main subindices, the perceived safety index, is based on survey data only and consists of three elements: risk perception, feelings of unsafety and avoidance:

- **Risk perception** is added to the index based on a model of perceived safety developed by Boers [6]. This model states that a part of the perceived safety of people can be explained by their perception of risk of becoming victim of crime and nuisance. Risk perception was measured by asking questions like '*Do you feel that there is a lot, little or no crime in your neighborhood?*' and '*Do you think crime in your neighborhood has increased, decreased, or stayed the same in the past 5 months?*'
- **Feelings of unsafety** are measured by asking questions about feeling unsafe in general, in the own neighborhood, at street in the evening and when home alone. In addition to this, respondents are asked if they are afraid to become a victim of crime and to provide a grade for the safety of their own neighborhood.
- **Avoidance** is added to the index because acting on feelings of unsafety goes one step further than just experiencing these feelings. It is measured by asking questions such as '*Does it ever occur to you to detour or drive around your own neighborhood to avoid unsafe places?*'

The answers to the questions are again converted to a 100 point scale, made comparable between neighborhoods and indexed relative to the base year 2014. The resulting index is then as follows:

$$\text{Perceived safety index} = \frac{1}{3} \times \text{Risk perception index} + \frac{1}{3} \times \text{Feelings of unsafety} + \frac{1}{3} \times \text{Avoidance index}$$

4.2. Applying Our Methodology to Amsterdam

This section will outline the specifics on how we applied our methodology to the target area: Amsterdam.

4.2.1. Included Neighborhoods

Due to the limited budget available for this project, data was collected on a subset of 43 of the 104 neighborhoods. The neighborhoods were selected to represent a variety of different scores on the Amsterdam Safety Index, while being geographically connected. These neighborhoods, along with their population and index values for the main safety index and its three subindices can be found in Table 4.1.

4.2.2. Hardware and Software

The whole pipeline was written and tested in Python 3.9 and is publicly available on GitHub². The code for the facade labeling algorithm by Li et al. [30] and the geolocalization algorithm by Qiu et al. [41, 48] was provided by the authors on their publicly available GitHub pages³⁴ and adapted to take input from and produce output for the pipeline. All other software dependencies are available from PyPI and are listed in the requirements.txt file on the GitHub repository.

The experiment was conducted on a MacBook Air mid 2013 model with 8GB of RAM and a Intel Core i7 chip with integrated Intel HD Graphics 5000. Using this setup, running all steps of the pipeline took up to several hours per neighborhood depending on its size.

4.2.3. Data Collection

We obtained the polygons representing the geographic barriers of each neighborhood in Table 4.1 from the municipality of Amsterdam. The building footprints and street network for each neighborhood were then obtained as described in Section 3.2. A total of 6 667 street segments were retrieved.

In total, 109 988 images were retrieved from the Google Street View Static API. All the images had the maximum allowed resolution of 640x640 pixels. The *field of view* parameter was set to 90 and the *pitch* parameter was set to 0. All indoor images were excluded by setting the *source* parameter to *outdoor*.

Within these images, a total of 872 360 building openings were detected and geolocalized. For the facade labeling algorithm, the best performing model, the ResNet18 model, was used in this experiment. For the height of the Google Street View camera, 2.5 meters is used.

4.2.4. Calculating Road Surveillability and Occupant Surveillability

As previously described in Section 3.2.3, the calculation of the road surveillability and occupant surveillability features is dependent on three variables: the maximum altitude of the windows included, a_{max} , the maximum length of the sightlines included, d_{max} , and the field of view of the windows, θ_{fov} .

Based on the finding by Lee et al. [29] that visibility from ground floor windows has a greater diminishing effect on street crime than higher story windows we calculate our features including building openings at different levels. We follow the rule of thumb that a story is 3 meters high, and calculate the features including only first-floor building openings (in short **1F**) with $a_{max} = 3m$, first and second-floor openings (**≤2F**) with $a_{max} = 6m$ and first, second and third-floor openings (**≤3F**) with $a_{max} = 9m$.

The literature review on eye-witness literature by Amiri [1, 18, 23, 31, 33, 36], concluded that 15 meters was the most **reliable** distance for observing and interpreting an event. Events witnessed from 43 meters yielded diminished yet **dependable** eye witness accounts. We therefore calculate our features with both $d_{max} = 15m$ and $d_{max} = 43m$.

The field of view, θ_{fov} , is constant throughout the experiment and set to 90 degrees (thus 45 degrees to the left and 45 degrees to the right). Combining this results in 6 configurations for both the occupant and road surveillability feature: 1F reliable, 1F dependable, ≤2F reliable, ≤2F dependable, etc.

²Code for the data pipeline on GitHub: <https://github.com/timovanasten/natural-surveillance>

³Window Detection in Facades Using Heatmaps Fusion on GitHub: https://github.com/lck1201/win_det_heatmaps

⁴Geolocalization algorithm on GitHub: https://github.com/shahinsharifi/AutoMap/tree/dev/location_estimator

4.2.5. Correlation with the Amsterdam Safety Index

To investigate the relationship between safety and natural surveillance as measured in our methodology, we correlate the occupant surveillability and road surveillability feature values with the Amsterdam Safety Index. We calculate the correlation between the main index as well as the subindices for crime, nuisance and perceived safety.

Correlation Metric

The correlation metric used to express this correlation is the Pearson correlation coefficient. This coefficient, denoted with the letter r , expresses the strength of a linear correlation with a number between -1 and 1. Here, -1 means a strong negative correlation, 1 means a strong positive correlation and 0 means no correlation exists between the two variables. The Pearson correlation coefficient is given by the following formula:

$$r_{xy} = \frac{n \sum x_i y_i - \sum x_i \sum y_i}{\sqrt{n \sum x_i^2 - (\sum x_i)^2} \sqrt{n \sum y_i^2 - (\sum y_i)^2}}$$

Here, x_i and y_i are the samples of the variables to be correlated, for example, occupant surveillability and the safety index, and n is the number of samples, which in our case is the number of neighborhoods.

Accounting for COVID

The most recently published data for the safety index is from 2020. However, 2020 was a year full of restrictions and lockdowns due to the COVID19 pandemic, which also affected crime. Besides 2020, we therefore also provide the correlations with the 2019 index.

Table 4.1: List of neighborhoods included in the experiment, including their safety according to the Amsterdam Safety Index 2020. The neighborhoods are listed from unsafer to safer. For reference, the region average on the index in 2020 was 96.

Neighborhood	Population	Safety index	Crime	Nuisance	Perceived safety
Burgwallen-Oude Zijde	4465	178	125	285	124
Burgwallen-Nieuwe Zijde	4134	166	88	293	116
Slotermeer-Zuidwest (area code F77abe)	6440	148	128	176	140
Osdorp-Oost	5436	141	112	148	163
Slotermeer-Noordoost	9703	134	109	146	146
De Punt	9275	127	92	146	144
Slotermeer-Zuidwest (area code F77cdf)	7480	124	98	142	131
Osdorp-Midden	13098	119	91	122	145
Eendracht	19600	114	84	113	144
Da Costabuurt	10724	113	111	139	91
Oude Pijp	10435	110	77	160	92
Zuid Pijp	9480	109	74	142	111
Landlust	16676	104	85	129	99
Van Lennepbuurt	8137	100	73	133	95
Overtoomse Veld	10811	100	74	110	115
Van Galenbuurt	14034	99	66	131	101
Hoofdweg e.o.	14812	99	76	129	92
Weesperzijde	8196	98	97	122	75
Grachtengordel-Zuid	5516	97	65	156	70
De Weteringschans	12619	97	65	158	69
Kinkerbuurt	11925	96	81	118	89
De Kolenkit	8537	95	67	115	103
Jordaan	13613	94	81	131	70
Nieuwmarkt/Lastage	5894	92	72	129	74
Nieuwe Pijp	9237	91	61	127	84
Erasmuspark	4704	90	77	95	98
Helmersbuurt/Vondelbuurt	15730	90	78	116	75
Frederik Hendrikbuurt/Centrale Markt	8264	89	75	106	86
IJselbuurt	11637	89	79	107	81
Slotervaart-Zuid	3234	87	56	98	107
Chassébuurt	9561	87	65	103	93
Slotervaart-Noord	8554	86	51	94	113
Geuzenbuurt	11958	86	81	89	89
Grachtengordel-West	13191	85	45	127	83
Museumkwartier	11154	85	73	106	75
Westindische Buurt	14781	84	78	92	82
Staatsliedenbuurt	3455	81	68	99	75
Willemspark	10765	78	75	83	77
Overtoomse Sluis	1620	73	61	86	73
Rijnbuurt	9336	74	32	102	89
Schinkelbuurt	20535	68	44	101	60
Scheldebuurt	13135	67	50	81	69
Buitenveldert-West	5170	62	45	61	82

5

Results

This chapter will present the results of applying our methodology to Amsterdam. These results aim to provide an answer to **RQ2**: 'How do the measurements produced by the proposed methodology relate to the (perceived) safety of an urban area?'. It will present the calculated feature values per neighborhood for both occupant and road surveillability. In addition to this, the correlations of these features with the Amsterdam Safety Index and its subindices will be presented. To make these relationships more visual, we present the data in the form of scatter plot matrices (SPLOMs). Lastly, to make an assessment of the correctness of the natural surveillance scores, we provide color coded maps of three neighborhoods, which include several snapshots of street level imagery.

5.1. Road Surveillability

For each of the 43 neighborhoods included in the experiment, the obtained values for the road surveillability feature (as explained in Section 3.2.3) can be found in Table 5.1.

The Pearson correlations of feature values with the Amsterdam Safety Index and subindices for both 2019 (pre-COVID) and 2020 (COVID) and can be found in Table 5.2. The strongest statistically significant correlation per (sub)index is highlighted in bold. A visual representation of these relationships with the 2019 version of the index can be found in Figure 5.1.

The two tables and the figure contain the values calculated for the 6 configurations for the included floors and maximum lengths of the sightlines included in the feature value as explained in Section 4.2.4, along with one extra configuration where all detected sightlines were included.

A multitude of statically significant relationships were found. For the 2019 safety index, all feature configurations had a **significant negative correlation** with the overall index, with the index being most strongly correlated with the 1F dependable feature ($r = -0.53, p < .001$). This means that as a neighborhood has more (detected) sightlines between the street and building openings, the neighborhood tends to be safer according to the index. When looking at the subindices of the safety index, statistically relevant correlations were found with perceived safety, nuisance and crime (more specifically high impact crime). Interestingly, the relationships with High Impact Crime only exist with the 2019 index and not in the 2020 index.

5.2. Occupant Surveillability

We present the feature values and correlations for the occupant surveillability feature (as explained in Section 3.2.3) in a similar manner to those of the road surveillability feature. The obtained feature values can be found in Table 5.3. The correlations with the Amsterdam Safety Index can be found in Table 5.4. A visual representation of these relationships with the 2019 version of the index can be found in Figure 5.2.

The occupant surveillability feature had multiple statistically significant negative correlations with the Amsterdam Safety Index and its subindices. However, these were less strong than those of the road surveillability feature and had higher p values ($p < .05$ vs $p < .001$ for road surveillability). Safety index values that significantly correlated with occupant surveillability include the main safety index, High Impact Crime, nuisance

(2020 only), and perceived safety (2020 only).

5.3. Manual Assessment

To get a feeling for how the produced scores compare to the actual situation at street level, we manually investigated some of the street segments for three neighborhoods: *Pijp Zuid*, which overall scores high on natural surveillance, *Osdorp-Oost*, which scores mediocre, and *De Punt*, which scores low. For this, we looked at the feature most correlated with overall safety: the *road surveillability 1F dependable* feature. Maps of these three areas, along with street view imagery of some of the investigated street segments are presented in Figure 5.3, Figure 5.4 and Figure 5.5.

Table 5.1: Feature values for the road surveillability feature for each of the included neighborhoods.

Neighborhood	Road surveillability feature values						
	Maximum sightline length			Included floors			
	15m (reliable)			43m (dependable)			None
	1F	≤2F	≤3F	1F	≤2F	≤3F	All
Burgwallen-Oude Zijde	0.07	0.29	0.39	0.12	0.55	0.91	1.35
Burgwallen-Nieuwe Zijde	0.09	0.37	0.63	0.11	0.60	1.15	1.32
Slotermeer-Zuidwest (F77abe)	0.10	0.28	0.33	0.16	0.46	0.60	0.64
Osdorp-Oost	0.12	0.33	0.41	0.17	0.63	0.89	1.09
Slotermeer-Noordoost	0.15	0.34	0.42	0.18	0.53	0.71	0.76
De Punt	0.10	0.26	0.30	0.14	0.42	0.52	0.58
Slotermeer-Zuidwest (F77cdf)	0.14	0.35	0.44	0.23	0.69	1.02	1.11
Osdorp-Midden	0.10	0.30	0.44	0.19	0.60	0.97	1.07
Eendrecht	0.12	0.31	0.37	0.14	0.42	0.53	0.54
Da Costabuurt	0.16	0.59	0.97	0.19	0.97	1.73	2.79
Oude Pijp	0.23	0.82	1.26	0.26	1.05	1.71	1.87
Zuid Pijp	0.32	0.80	1.09	0.40	1.07	1.54	1.65
Landlust	0.17	0.54	0.81	0.28	0.98	1.58	1.73
Van Lennepbuurt	0.23	0.80	1.29	0.25	0.92	1.55	2.00
Overtoomse Veld	0.07	0.21	0.30	0.13	0.43	0.68	1.07
Van Galenbuurt	0.20	0.70	1.09	0.29	1.26	2.10	2.31
Hoofdweg e.o.	0.31	0.95	1.40	0.43	1.50	2.42	3.17
Weesperzijde	0.19	0.51	0.74	0.23	0.65	1.01	1.47
Grachtengordel-Zuid	0.16	0.43	0.53	0.18	0.52	0.70	0.96
De Weteringschans	0.13	0.38	0.55	0.16	0.51	0.81	0.88
Kinkerbuurt	0.29	0.84	1.17	0.32	0.98	1.42	1.84
De Kolenkit	0.10	0.29	0.46	0.17	0.55	0.92	1.46
Jordaan	0.24	0.59	0.72	0.36	1.03	1.43	1.71
Nieuwmarkt/Lastage	0.08	0.23	0.34	0.12	0.44	0.76	0.85
Nieuwe Pijp	0.31	0.93	1.38	0.36	1.21	1.92	2.09
Erasmuspark	0.17	0.55	0.84	0.33	1.10	1.83	2.04
Helmersbuurt/Vondelbuurt	0.23	0.69	1.09	0.31	1.09	1.89	2.11
Frederik Hendrikbuurt/Centrale Markt	0.27	0.77	1.15	0.35	1.10	1.77	1.96
IJselbuurt	0.28	0.73	1.02	0.33	0.97	1.45	2.02
Slotervaart-Zuid	0.10	0.23	0.31	0.16	0.50	0.71	0.76
Chassébuurt	0.29	0.84	1.18	0.34	1.03	1.52	1.68
Slotervaart-Noord	0.14	0.30	0.34	0.18	0.46	0.56	0.59
Geuzenbuurt	0.29	0.88	1.38	0.35	1.14	1.84	2.02
Grachtengordel-West	0.13	0.29	0.35	0.15	0.37	0.50	0.63
Museumkwartier	0.26	0.66	1.02	0.33	0.92	1.49	1.66
Westindische Buurt	0.18	0.57	0.86	0.30	1.05	1.69	1.87
Staatsliedenbuurt	0.35	1.01	1.40	0.40	1.16	1.66	2.03
Willemspark	0.25	0.65	0.95	0.34	0.93	1.45	2.06
Overtoomse Sluis	0.24	0.72	1.03	0.28	0.95	1.46	2.00
Rijnbuurt	0.19	0.60	0.81	0.34	1.11	1.65	1.80
Schinkelbuurt	0.18	0.58	0.87	0.19	0.73	1.18	1.67
Scheldebuur	0.21	0.60	0.87	0.30	0.96	1.50	1.98
Buitenveldert-West	0.06	0.22	0.31	0.12	0.46	0.72	0.97

Table 5.2: Pearson correlations of the road surveillability feature with the Amsterdam Safety Index 2019 and 2020.
^{*} = $p \leq .05$, ^{**} = $p \leq .01$, ^{***} = $p \leq .001$

Correlations of road surveillability with the Amsterdam Safety Index							
Index and subindices	Maximum sightline length						None
	15m (reliable)			43m (dependable)			
	1F	≤2F	≤3F	1F	≤2F	≤3F	All
2019 (Pre-COVID)							
Safety Index	-0.48**	-0.44**	-0.43**	-0.53***	-0.48**	-0.42**	-0.42**
Crime	-0.29	-0.32*	-0.31*	-0.37*	-0.42**	-0.39*	-0.37*
<i>High Impact Crime</i>	-0.36*	-0.41**	-0.42**	-0.37*	-0.45**	-0.45**	-0.53***
<i>High Volume Crime</i>	-0.15	-0.15	-0.13	-0.25	-0.26*	-0.21	-0.12
Nuisance	-0.36*	-0.27	-0.25	-0.41**	-0.3*	-0.23	-0.22
<i>Nuisance by people</i>	-0.33*	-0.24	-0.22	-0.39**	-0.27*	-0.2	-0.18
<i>Deterioration</i>	-0.41**	-0.39**	-0.38*	-0.43**	-0.42**	-0.38*	-0.37*
Perceived Safety	-0.52***	-0.55***	-0.56***	-0.47**	-0.47**	-0.48**	-0.53***
<i>Risk perception</i>	-0.46**	-0.42**	-0.41**	-0.51***	-0.45**	-0.41**	-0.41**
<i>Feelings of unsafety</i>	-0.43**	-0.46**	-0.46**	-0.39**	-0.4**	-0.41**	-0.46**
<i>Avoidance</i>	-0.49***	-0.54***	-0.55***	-0.41**	-0.43**	-0.45**	-0.49***
2020 (COVID)							
Safety Index	-0.41**	-0.37*	-0.36*	-0.44**	-0.34*	-0.3*	-0.3*
Crime	-0.21	-0.19	-0.18	-0.21	-0.16	-0.13	-0.09
<i>High Impact Crime</i>	-0.2	-0.17	-0.17	-0.19	-0.09	-0.08	-0.06
<i>High Volume Crime</i>	-0.11	-0.13	-0.11	-0.14	-0.18	-0.15	-0.09
Nuisance	-0.33*	-0.25	-0.22	-0.39**	-0.25	-0.19	-0.19
<i>Nuisance by people</i>	-0.31*	-0.22	-0.19	-0.38*	-0.24	-0.18	-0.17
<i>Deterioration</i>	-0.3	-0.27	-0.27*	-0.29	-0.22	-0.19	-0.19
Perceived Safety	-0.46**	-0.49***	-0.5***	-0.42**	-0.42**	-0.44**	-0.49***
<i>Risk perception</i>	-0.39**	-0.38*	-0.39**	-0.43**	-0.4**	-0.4**	-0.43**
<i>Feelings of unsafety</i>	-0.48**	-0.5***	-0.51***	-0.44**	-0.43**	-0.44**	-0.49***
<i>Avoidance</i>	-0.43**	-0.47**	-0.48**	-0.37*	-0.39*	-0.41**	-0.47**

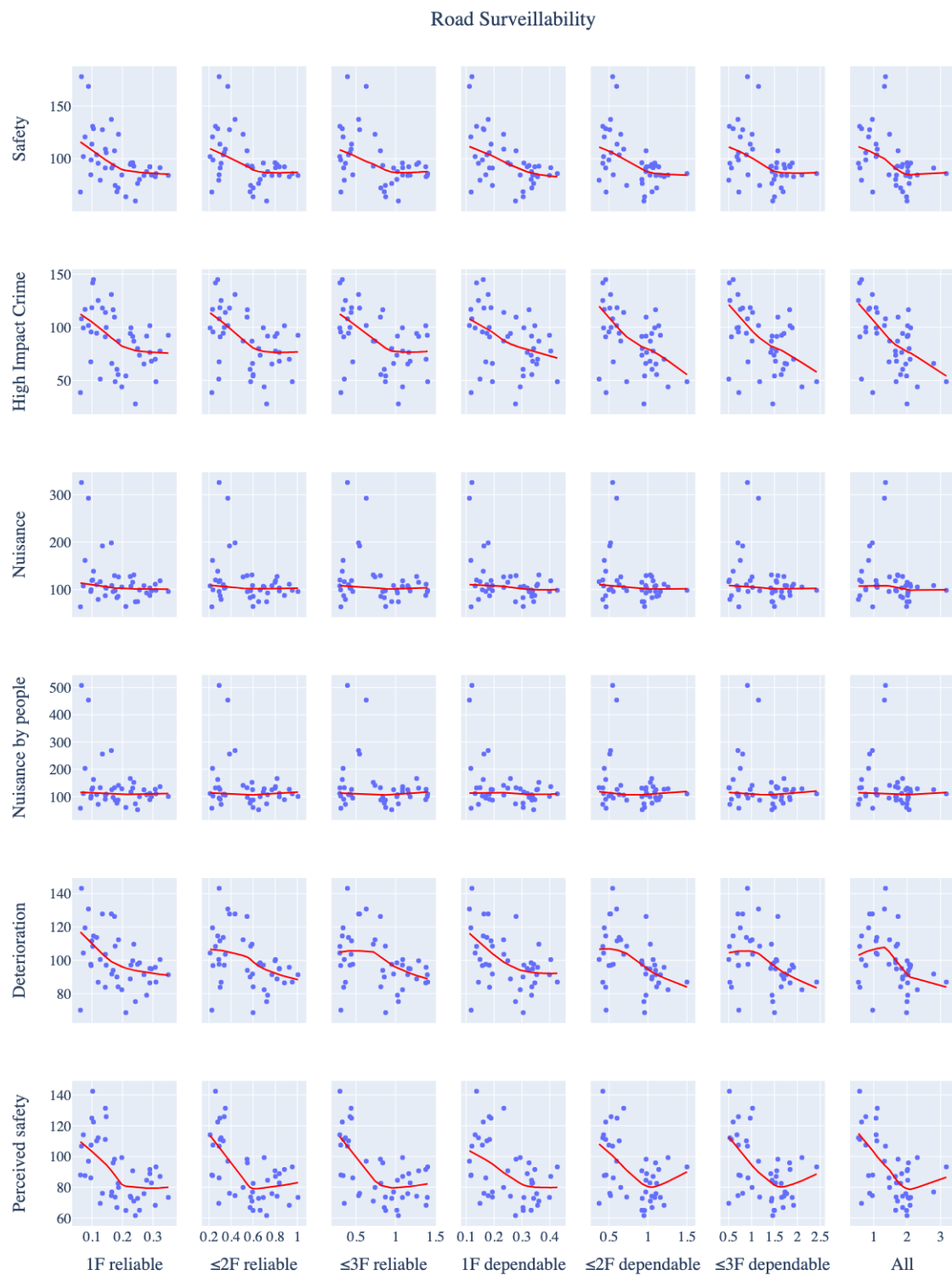


Figure 5.1: Scatter plot matrix with LOWESS trendlines of the road surveillability features (x-axis) and the Amsterdam Safety Index (y-axis).

Table 5.3: Feature values for the occupant surveillability feature for each of the included neighborhoods.

Neighborhood	Occupant surveillability feature values					
	Maximum Sightline Length			Included Floors		
	15m (reliable)		43m (dependable)	1F	≤2F	≤3F
Burgwallen-Oude Zijde	0.15	2.22	5.84	0.82	13.20	42.39
Burgwallen-Nieuwe Zijde	0.22	2.81	9.80	0.80	15.99	59.88
Slotermeer-Zuidwest (area code F77abe)	1.17	8.41	16.23	3.96	30.12	55.92
Osdorp-Oost	0.25	3.48	8.37	1.07	13.80	30.89
Slotermeer-Noordoost	0.35	2.39	5.69	1.06	9.07	18.68
De Punt	0.19	1.65	2.56	0.76	6.52	10.45
Slotermeer-Zuidwest (area code F77cdf)	0.54	4.37	12.34	2.20	18.76	47.54
Osdorp-Midden	0.59	4.60	13.99	1.79	16.80	48.50
Eendracht	0.16	1.11	1.56	0.60	5.18	8.25
Da Costabuurt	0.53	7.39	24.11	1.51	35.44	128.83
Oude Pijp	0.61	6.55	17.12	2.22	30.99	86.71
Zuid Pijp	1.00	6.00	13.09	4.82	33.47	76.87
Landlust	0.82	7.51	22.41	3.55	34.91	98.04
Van Lennebuurt	0.57	5.84	19.63	2.56	26.32	79.31
Overtoomse Veld	0.21	1.42	3.80	0.88	6.54	15.84
Van Galenbuurt	0.69	11.64	32.07	4.33	84.04	230.05
Hoofdweg e.o.	1.53	14.98	40.24	8.85	97.23	265.88
Weesperzijde	1.32	4.84	9.64	2.56	15.02	33.65
Grachtengordel-Zuid	0.88	7.63	14.71	2.57	24.63	48.70
De Weteringschans	0.30	2.36	5.95	0.82	8.75	24.16
Kinkerbuurt	2.10	17.25	37.36	8.30	74.22	164.01
De Kolenkit	0.39	3.19	8.73	1.68	13.05	33.52
Jordaan	2.15	12.14	22.56	6.39	53.21	116.71
Nieuwmarkt/Lastage	0.15	2.55	8.99	0.62	10.36	35.51
Nieuwe Pijp	0.97	8.11	20.87	4.15	40.90	106.48
Erasmuspark	1.84	12.29	34.32	10.38	74.44	200.02
Helmersbuurt/Vondelbuurt	1.10	9.87	30.14	5.41	57.15	179.47
Frederik Hendrikbuurt/Centrale Markt	1.34	10.81	29.91	5.21	51.38	143.69
IJselbuurt	0.86	6.38	15.50	3.75	33.04	85.72
Slotervaart-Zuid	0.31	2.22	5.43	1.09	8.88	20.39
Chassébuurt	0.72	5.37	13.15	3.83	33.31	81.99
Slotervaart-Noord	1.17	6.51	10.38	4.28	25.11	38.59
Geuzenbuurt	1.02	6.98	18.44	5.92	42.95	118.26
Grachtengordel-West	0.17	1.10	2.18	0.44	3.24	6.82
Museumkwartier	1.01	6.42	16.90	5.09	34.47	91.91
Westindische Buurt	0.74	8.08	22.06	3.30	41.83	114.29
Staatsliedenbuurt	1.23	9.46	20.31	5.10	43.56	90.43
Willemspark	0.67	3.86	9.00	3.75	25.49	60.23
Overtoomse Sluis	0.71	7.37	19.05	2.52	30.10	78.70
Rijnbuurt	0.67	5.35	12.63	3.01	30.42	67.37
Schinkelbuurt	0.65	5.06	14.30	2.78	23.29	59.03
Scheldebuit	0.64	5.69	15.15	3.13	24.94	60.08
Buitenveldert-West	0.64	8.40	21.54	2.02	27.36	69.37

Table 5.4: Pearson correlations of the occupant surveillability feature with the Amsterdam Safety Index 2019 and 2020.
^{*} = $p \leq .05$, ^{**} = $p \leq .01$, ^{***} = $p \leq .001$

Correlations of occupant surveillability with the Amsterdam Safety Index						
Index and subindices	Maximum sightline length					
	15m (reliable)			43m (dependable)		
	1F	$\leq 2F$	$\leq 3F$	1F	$\leq 2F$	$\leq 3F$
2019 (Pre-COVID)						
Safety Index	-0.26	-0.33*	-0.34*	-0.34*	-0.33*	-0.3*
Crime	-0.04	-0.23	-0.28*	-0.19	-0.31*	-0.29
<i>High Impact Crime</i>	-0.12	-0.29*	-0.34*	-0.17	-0.34*	-0.35*
<i>High Volume Crime</i>	0.03	-0.11	-0.14	-0.15	-0.19	-0.16
Nuisance	-0.24	-0.24	-0.24	-0.3	-0.23	-0.18
<i>Nuisance by people</i>	-0.24	-0.22	-0.21	-0.28	-0.2	-0.15
<i>Deterioration</i>	-0.21	-0.33*	-0.34*	-0.31*	-0.35*	-0.33*
Perceived Safety	-0.28*	-0.3*	-0.31*	-0.25	-0.27	-0.28*
<i>Risk perception</i>	-0.22	-0.24	-0.27*	-0.28	-0.26	-0.24
<i>Feelings of unsafety</i>	-0.26*	-0.28*	-0.29*	-0.22	-0.24	-0.25
<i>Avoidance</i>	-0.26*	-0.27*	-0.28*	-0.21	-0.23	-0.25
2020 (COVID)						
Safety Index	-0.3	-0.28	-0.28	-0.32*	-0.25	-0.21
Crime	-0.03	-0.06	-0.06	-0.1	-0.08	-0.04
<i>High Impact Crime</i>	-0.04	0.01	0.02	-0.06	0.02	0.05
<i>High Volume Crime</i>	-0.0	-0.14	-0.14	-0.1	-0.18	-0.15
Nuisance	-0.28	-0.24	-0.23	-0.31*	-0.2	-0.15
<i>Nuisance by people</i>	-0.28	-0.24	-0.23	-0.32*	-0.21	-0.15
<i>Deterioration</i>	-0.16	-0.15	-0.14	-0.18	-0.12	-0.1
Perceived Safety	-0.35*	-0.36*	-0.36*	-0.32*	-0.32*	-0.32*
<i>Risk perception</i>	-0.32*	-0.35*	-0.39*	-0.31*	-0.29	-0.29
<i>Feelings of unsafety</i>	-0.35*	-0.36*	-0.36*	-0.33*	-0.32*	-0.31*
<i>Avoidance</i>	-0.33*	-0.34*	-0.33*	-0.29	-0.3*	-0.31*

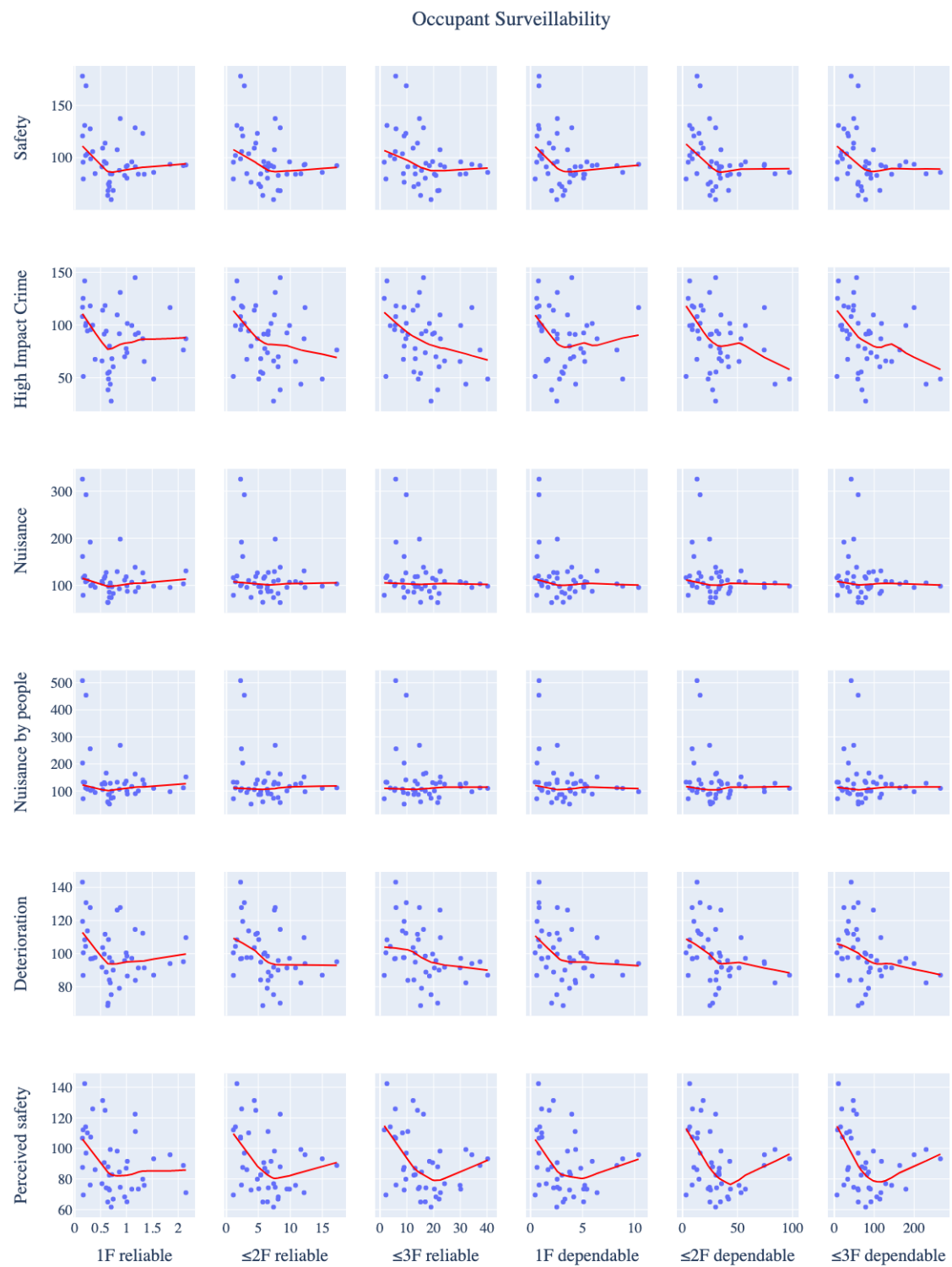


Figure 5.2: Scatter plot matrix with LOWESS trendlines of the occupant surveillability features (x-axis) and the Amsterdam Safety Index (y-axis).

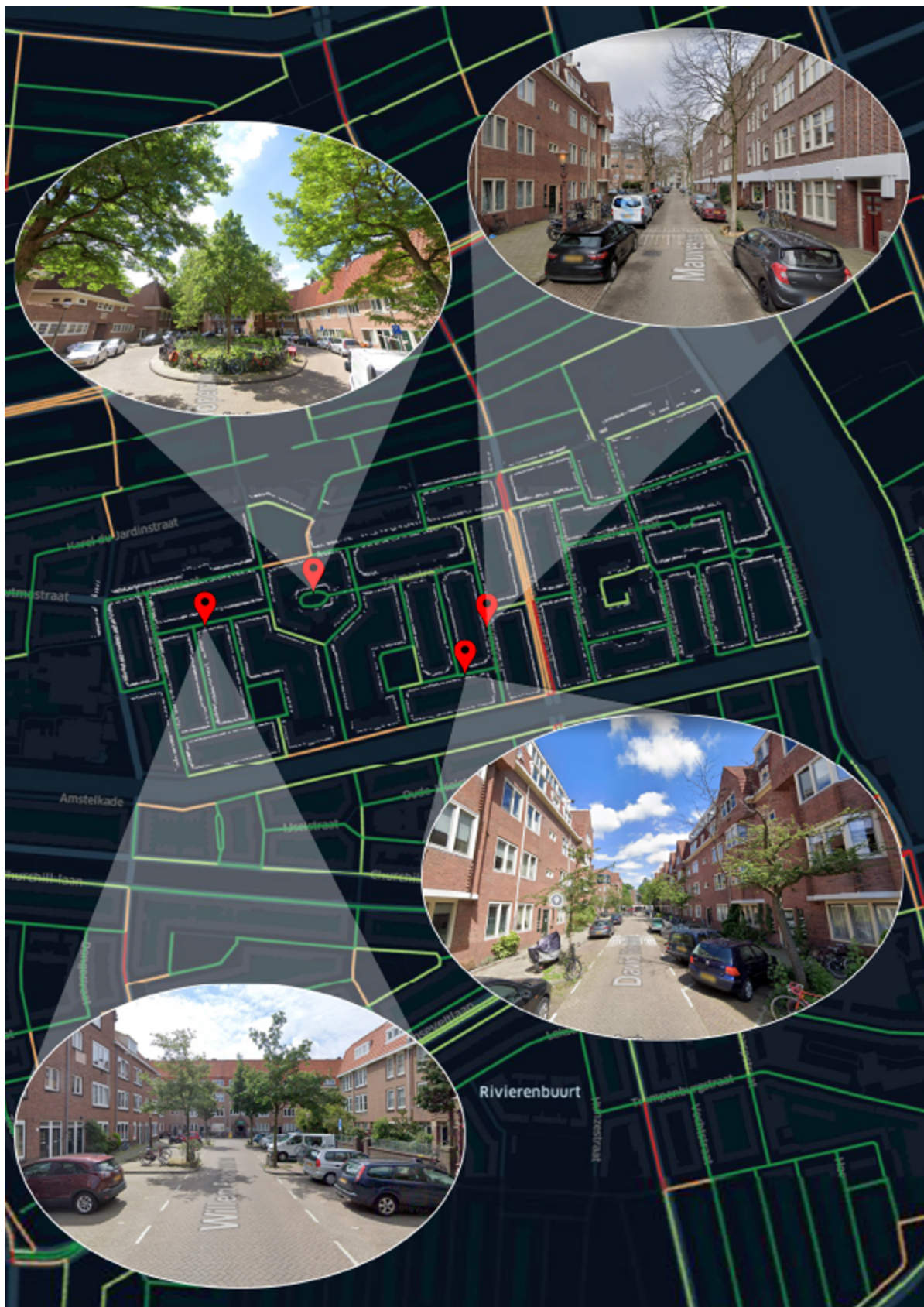


Figure 5.3: Map of the *road surveillability 1F dependable* feature for the neighborhood *Pijp-Zuid*, which on average scores high on natural surveillance. Street segments with a low natural surveillance score are shown red. Street segments with a high score are shown in green.



Figure 5.4: Map of the *road surveillability 1F dependable* feature for the neighborhood *Osdorp-Oost*, which on average scores mediocre on natural surveillance. Street segments with a low natural surveillance score are shown red. Street segments with a high score are shown in green.

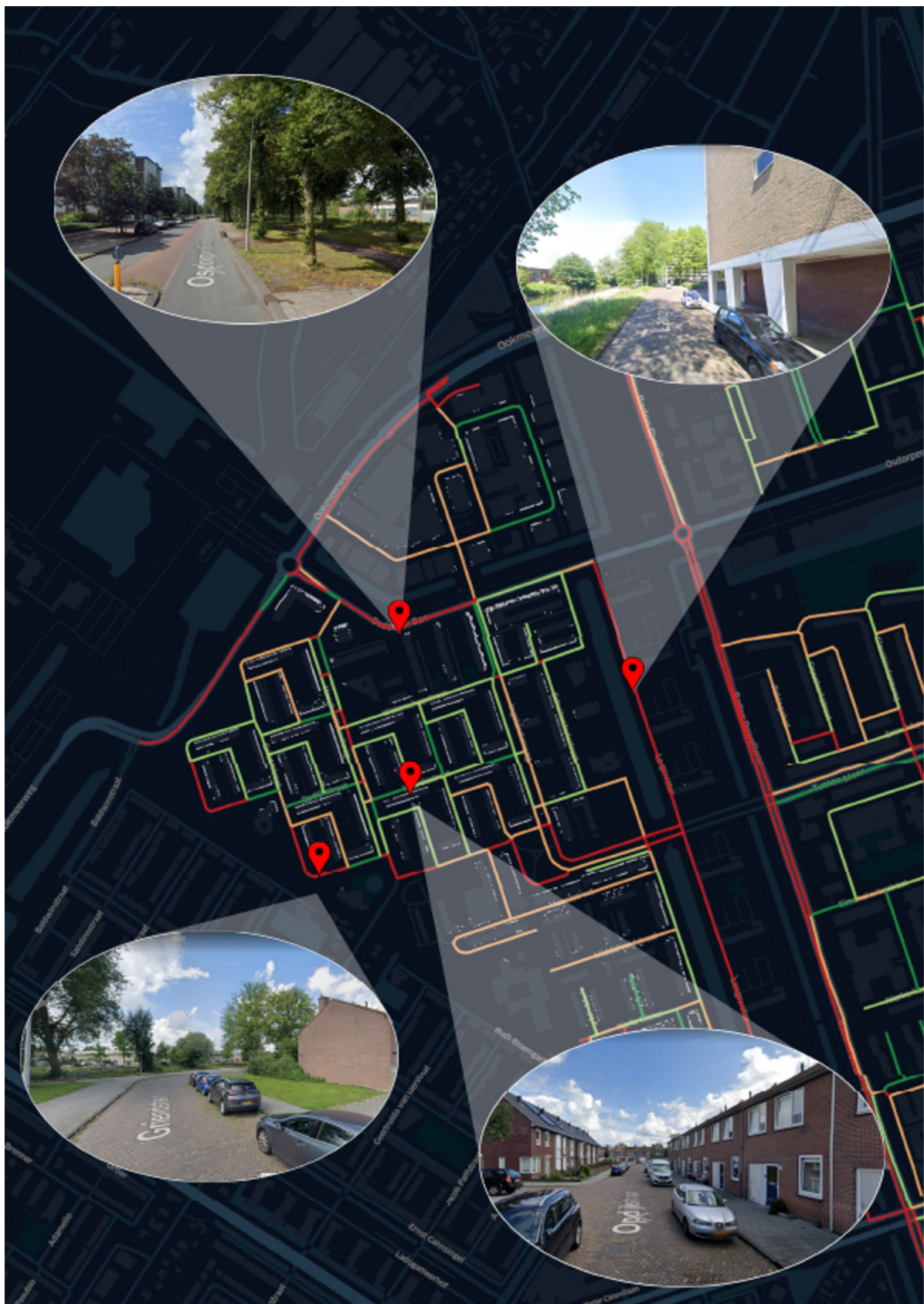


Figure 5.5: Map of the *road surveillability 1F dependable* feature for neighborhood *De Punt*, which on average scores low on natural surveillance. Street segments with a low natural surveillance score are shown red. Street segments with a high score are shown in green.

6

Discussion

In this chapter we will discuss the results of our experiment shown in Chapter 5 as well as the strengths and limitations of the methodology used to obtain them as outlined in Chapter 3.

6.1. Discussion of Experiment Results

First, we try to provide an answer to **RQ2**: 'How do the measurements produced by the proposed methodology relate to the (perceived) safety of an urban area?'. It should be noted that because the experiment had a correlational design, all limitations of a correlational research apply and should be considered when reading this section.

When studying our data, it becomes clear that most of our computed features are **significantly and negatively correlated** with the Amsterdam Safety Index. Since the index has lower values as the neighborhood becomes safer, this means that **as the average natural surveillance (as measured by our method) in a neighborhood increases, the neighborhood tends to be safer**. This is in line with what would be expected according to the CPTED literature discussed in Chapter 2. The correlations were stronger for the road surveillability features than the occupant surveillability features, which could suggest that road surveillability plays a bigger role in the overall safety of a neighborhood than occupant surveillability.

Furthermore, significant correlations were found with all 3 subindices of the main index: crime, nuisance and perceived safety. Here, perceived safety seems to be the most correlated ($r_{max} = -0.56, p < .001$), followed by crime ($r_{max} = -0.42, p = .006$) and nuisance ($r_{max} = -0.41, p = .006$).

When looking further at the subindices, one interesting observation is that while high impact crime (i.e. (street) robbery, violence, threatening, murder, sex crimes etc.) was significantly correlated with the natural surveillance features ($r_{max} = -0.56, p < .001$), this is not the case for high volume crime (i.e. theft, shoplifting, pick pocketing etc.). This could indicate that natural surveillance only has a deterring effect on high impact crimes and not on high volume crimes.

In the remainder of this section we will discuss further notable patterns found when analyzing the data.

6.1.1. Differences in Included Floor Levels and Sightline Lengths

When looking at differences in correlations for features including different level floors, a few interesting observations can be made. First, when looking at the High Impact Crime subindex, the correlations become stronger when including more floor levels into the feature calculation. A possible explanation for this could be that criminals are more deterred by being surrounded by high buildings with a multitude of possible observation points.

Interestingly enough an opposite was observed when looking at the nuisance subindex. Here, the relationship became stronger when excluding upper level floors. For the perceived safety subindex, the number of included floors did not seem to have a significant affect on the observed correlations.

Lastly, when looking differences between the features including and excluding sightlines longer than 15 meters long, no clear patterns were observed.

6.1.2. Differences Between the 2019 and 2020 Safety Index

The patterns observed in the 2019 (pre-COVID) and 2020 (COVID) version of the index are largely the same with one notable exception. The clear correlation between the natural surveillance features and High Impact Crime observed in the 2019 version of the index is not present in the 2020 version of the index. The most likely explanation for this would be the COVID measures in place during this year, which inhibited people (and criminals) to freely roam the streets. This is also visible in the Amsterdam Safety Index, which showed a strong decline in High Impact Crime during 2020.

6.1.3. Non-linear Relationship

An interesting observation can be made when looking at the trendlines in the data as shown in Figures 5.1 and 5.2. From this data it seems to be the case that the relationship of our natural surveillance features with safety is non-linear. Generally speaking, safety seems to increase with higher natural surveillance, up to a certain point where extra natural surveillance does not seem to be associated with lower scores on the safety index (where lower is safer). We will illustrate this based on the *road surveillability 1F reliable* feature, although the other features follow a similar trend. The pivot point in the trend line for this feature is present around a value of 0.2. For this feature that would mean that, on average, a 10 meter long section of street would have 2 (detected) first-story building openings overlooking it. Neighborhoods in Amsterdam that are close to such an average include the Van Galenbuurt and Oude Pijp. Any further increase, for example 7 building openings overlooking every 10 meters of street, does not seem to correlate with any further increase in neighborhood safety.

To give a visual indication of where this pivot point is located, Figure 6.1 provides examples of streets in the dataset that have scores of 0.0, 0.1, 0.2 and 0.7 for this feature. It should be noted, however, that because the trend was observed as an average at neighborhood level, this might not translate one to one to the scores at street level. Investigating these relationships at street level could yield different results.

6.2. Discussion of the Methodology

In Chapter 3, we presented a methodology to answer **RQ1**: 'How can the notion of natural surveillance be measured in a scalable way?'. In this section, we will discuss its ability to do so, the limitations of the methodology and some recommendations on how it could be improved.

6.2.1. Ability to Capture the Notion Natural Surveillance at Scale

Our methodology aims to capture the notion of natural surveillance at scale by detecting points from which the street can possibly be observed. From investigating the scores produced by our method, as shown in Figure 5.3-5.5, it seems to do a good job at this. Low scoring segments indeed seem to have a low number of building openings overlooking them and include elements such as dead walls, fencing or vegetation blocking sight upon the street. Meanwhile, high scoring streets seem to be well observed.

While this does capture a big portion of Jane Jacobs' original idea, natural surveillance is a broader concept that does encompass more than just possible observation points. Things like lighting and the presence of people on the streets are not captured by our method while these are factors that can contribute to natural surveillance. Furthermore, the studies that focussed on natural surveillance from which the two used metrics (road surveillability and occupant surveillability) were derived have mainly done so in the context of burglary target selection [1, 7, 28, 35, 37]. It is possible that a different operationalization can be contrived, which can capture the concept of natural surveillance better in the context of the general safety of a neighborhood.

On the aspect of scalability, our method has demonstrated to scale well. Computation times are reasonable and different areas can be computed in parallel, further reducing the time needed to obtain data. The method could therefore be applied to multiple cities and towns in multiple countries to see if a similar or different pattern emerges. Furthermore, the methodology does not require physical presence in the studied areas. The biggest limitation to the scalability of the method would be the costs associated with the Google Street View API, although these are not particularly high and the presented research was done using only the free

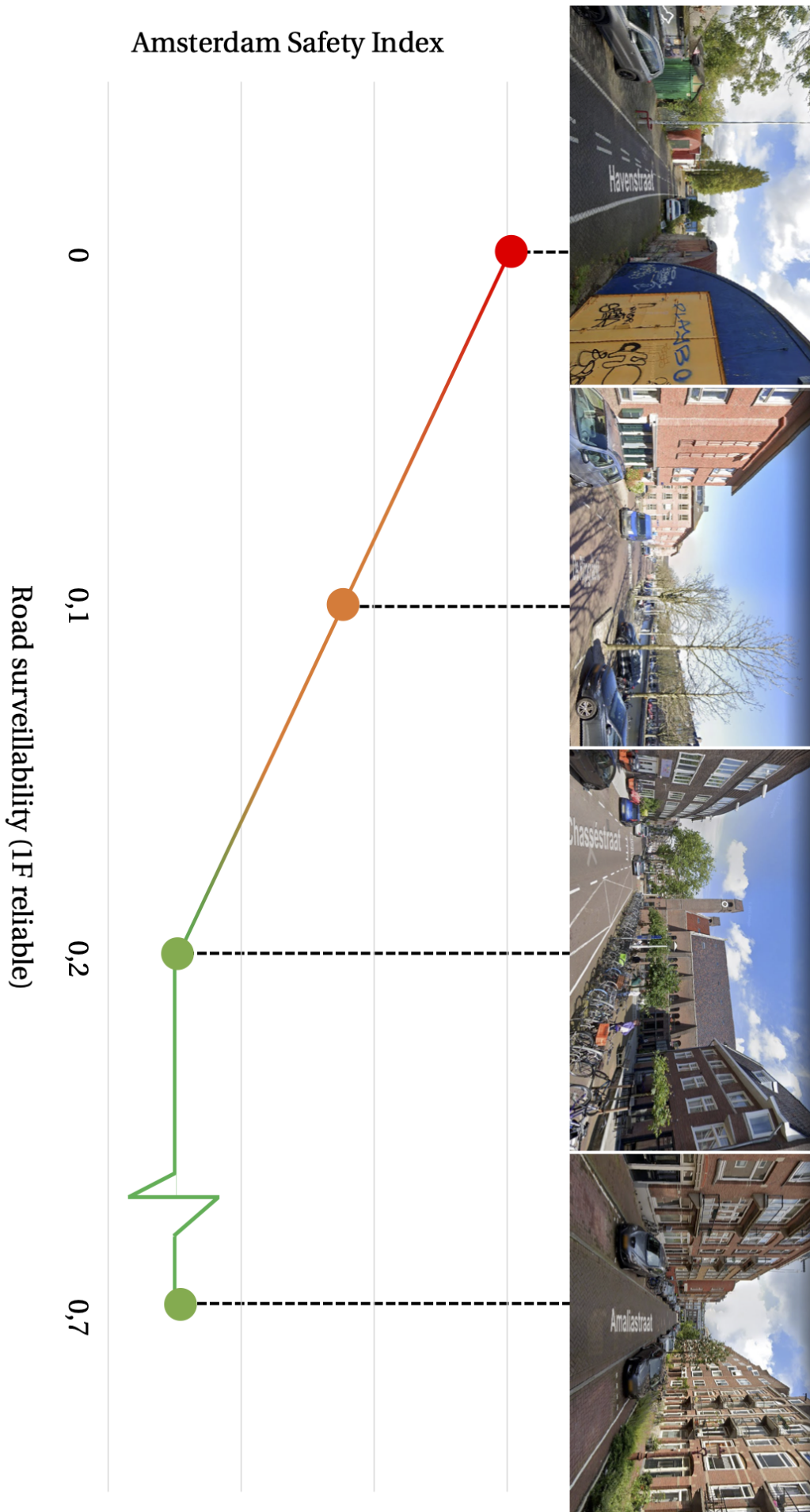


Figure 6.1: Selection of streets in Amsterdam along with their feature values for the *road surveillability 1F reliable* feature. The shown streets are, from left to right: Havenstraat, De Rijpgracht, Chasséstraat and Amaliastraat. A neighborhood tends to be safer as its average value rises to the 0.2 level, such as the Chasséstraat in this Figure. Further increase, such as to the 0.7 score of the Amaliastraat, does not seem to be correlated with increased safety.

credit provided by Google. When the availability of free street level imagery increases with platforms such as Mapillary, switching to a free platform as datasource in the future could make collecting data using our methodology as good as free.

6.2.2. Technical Limitations

The used methodology brings with it some technical limitations related to the facade labeling algorithm, the localization algorithm and their input data.

First of all, the use of street level imagery introduces the limitation that the streets can only be observed from a limited number of viewpoints. Consequently, some building openings are not visible in the street level imagery, either because they are blocked or because no imagery is present for that particular part of the street. In the evaluation of our method, this was the case for 12% of the building openings. Also, privacy blurs and distortions are occasionally present in the Google Street View data, preventing some openings from being detected. Furthermore, in narrow streets, the camera of the Street View camera is very close to the facades. Because we kept the *pitch* parameter of the Google Street View API constant at 0, upper level windows are not present in the imagery for such streets. Narrow streets might therefore have a lower score for the features that include the upper level windows. It could however also be argued that it is harder to observe the streets from upper level windows in narrow streets, and this lower feature value is justified. The dependance of the method on building footprints also introduces the limitation that these should be up to both date, and accurate for the studied area to obtain accurate results.

Secondly, an important limitation is the accuracy of the used facade labeling algorithm. Although the algorithm performed well in our evaluation, detecting 83.3% of the visible openings, there are some situations in which it might not produce accurate results. Limitations mentioned by the authors [30] include reduced accuracy for openings in shadow, occluded openings and small openings. Furthermore, the algorithm was trained on residential building openings only, and thus storefronts are often not detected. However, these storefronts can provide natural surveillance in some cases. Although our evaluation showed good performance on street view imagery, it should be noted that the algorithm was not trained on such data. During our research we did encounter some algorithms that specifically aim to detect building openings in street level imagery [15, 24, 34]. While these authors did not provide implementations of their solutions, using one of their approaches or retraining the network used in the current approach could lead to more accurate results.

Lastly, the geolocalization algorithm can produce inaccurate results in some cases. As discussed earlier in Section 3.3.2, large errors in the estimated geolocation may arise if a building opening is projected onto the wrong building segment. Such an error can occur due to inaccuracies in the GPS metadata of the Google Street View imagery. Another cause is that the localization of building openings is done by first calculating an intersection with the building footprint in 2D, after which the altitude is calculated. A solution could be to instead execute the geolocalization step entirely in 3D. This would be possible by incorporating 3D models of buildings into the method. These models can already be generated for entire countries [14]. Question is if introducing such complexity would be worth solving this relatively small limitation. The last notable cause of error arises if a building opening is present in multiple street view images. In such a case, the same window can generate two entries in the dataset. Such an error can be mitigated by removing entries that are originating from different Street View images, but have a similar estimated geolocation.

6.3. Availability of Code and Data

To aid further research into the topic our code and data is publicly available at <https://github.com/timovanasten/natural-surveillance>.

7

Conclusion

In this concluding final chapter, we will present the study's main findings, discuss their contributions and value, and lastly, propose opportunities for possible future research.

7.1. Main Findings

7.1.1. Measuring Natural Surveillance in a Scalable Way

In this study, we studied natural surveillance: a type of surveillance that is a byproduct of how citizens normally and routinely use the environment. Previous studies have provided evidence that this concept plays a key role in the safety of urban areas. However, it is currently a very labour intensive and lengthy process to gather detailed data on this topic. This lack of data has been pointed out as a limitation in previous studies on urban safety.

To tackle this problem, we have aimed to develop a methodology to measure natural surveillance in a scalable way. The goal here was to provide researchers with a tool they can use to collect data that captures the essence of natural surveillance and can be applied to a study area of choice of any size.

We have first reviewed literature to pinpoint features that have previously been used to operationalize natural surveillance and identified what data would be needed to compute such features automatically and at scale. The two features that were chosen for this purpose were (1) road surveillability: the surveillability from buildings to the road and vice versa, and (2) occupant surveillability: surveillability between building openings. The data that was missing to compute such features at scale were the locations of building openings (i.e. windows and doors) throughout urban areas.

This has led us to design a system that can localize building openings in an urban area of choice in 3 dimensions. This was achieved by creating a pipeline that takes publicly available Google Street View and OpenStreetMap data and feeds this into facade labeling and geolocalization algorithms. We then evaluated the performance of this pipeline on a newly created ground truth dataset of building openings. This evaluation showed the pipeline to be able to provide 83% of visible building openings with a geolocalization that had a mean error of a 1.08m. This was deemed accurate enough for our research objective. From the estimated geolocations of building openings, our system was then able to compute road and occupant surveillability scores for every street segment in the area of choice and could aggregate these scores to provide a score for the entire area.

We then deployed our methodology on 43 neighborhoods in Amsterdam, which has demonstrated that **our method can scale to large areas and can collect data in a matter of hours** instead of months or even more than a year reported in previous research. To our knowledge, no research into natural surveillance has been conducted at such a large scale. Furthermore we manually checked a subset of streets to validate if the assigned score seems to accurately represent the amount of natural surveillance opportunities in the street. From this, it has become clear that **our method is able to produce scores that seem to capture the notion of natural surveillance as intended down to street segment level**.

7.1.2. Relationship Between Natural Surveillance and Safety

We then juxtaposed the natural surveillance scores for these 43 neighborhood to the Amsterdam Safety Index: an index that was designed to compare the safety of different neighborhoods on the aspects of crime, nuisance and perceived safety. The goal here was to identify how the computed natural surveillance scores relate to these aspects of urban safety. Analysis of this data has led to some interesting findings.

First of all, **our data indicates that as our natural surveillance scores for a neighborhood increase, the neighborhood tends to be safer**. This was true for both occupant surveillability and road surveillability, although the relationships were stronger for road surveillability. Furthermore, this relationship was observed for all the aspects of safety included in the index, meaning that **as our natural surveillance scores increased crime and nuisance decreased, and perceived safety increased**. For the relationship with crime, it was observed that **only high impact crime was significantly correlated with natural surveillance. For high volume crime, no significant relationship was observed**. All and all, these findings add further evidence for the importance of natural surveillance in urban safety.

Table 7.1: Summary of observed relationships.

Observed relationships	
Road surveillability	<ul style="list-style-type: none"> • Significantly correlated with increases in perceived safety of neighborhoods. • Significantly correlated with decreases in high impact crime and nuisance in neighborhoods.
Occupant surveillability	<ul style="list-style-type: none"> • Significantly correlated with the same elements as road surveillability, but did so less strongly.

Furthermore, an interesting effect was observed when it comes to the amount of natural surveillance that is associated with neighborhood safety increases. Our data shows evidence that **there is a threshold before which natural safety is related to safety increases, and after which additional natural surveillance does not seem to have any significant effect**. This effect is most noticeable in the perceived safety of a neighborhood. To our knowledge, this is a new finding not reported in previous literature. The exact value of this threshold differs depending on the floors and maximum sightline distance included in the calculation. As a guideline one could say this threshold lies around the point where, on average, every 10 meter section of street in a neighborhood is observed by two first floor windows within 15m of the road. For a visualization of this, please refer to Figure 6.1. However, since this is a neighborhood average, this value could be higher when looking at individual streets and is something that should be investigated further.

7.2. Future Work

First of all, the data generated by our method could be incorporated into safety indexes that cover other CPTED aspects, such as those developed by Shach-Pinsky [46, 47] who stated that such data had an important role in safety but was not available. By including such data, an index could be created that would give a more wholistic view on safety and could identify small hotspots where crime is more likely to occur.

Secondly, our method could be applied to other urban areas, in essence anywhere where the required input data is available. This could possibly create insights into the role natural surveillance plays in different kinds of urban areas (e.g. cities vs towns) or different countries.

Lastly, while our method is able to generate natural surveillance scores at the street segment level, our experiment was conducted at the neighborhood level because we had no access to crime or perceived safety data at the street level. With access to such data, it would be possible to investigate relationships between natural surveillance and safety at the street segment level. Such an approach is advocated by respectable criminology researchers such as David Weisburd, who claims that such an approach can yield "*significant new criminological insights that advance both theory and practical crime prevention*" [54].

Bibliography

- [1] Solmaz Amiri and Dennis R. Crain. Quantifying jacobs' notion of 'eyes upon the street' in 3-dimensions. *Journal of Urban Design*, 25(4):467–485, 2020. ISSN 1357-4809. doi: 10.1080/13574809.2019.1691440. URL <https://doi.org/10.1080/13574809.2019.1691440>.
- [2] Gemeente Amsterdam. Verantwoordingsdocument veiligheidsindex 2014. Report, 2015. URL <https://data.amsterdam.nl/publicaties/publicatie/verantwoordingsdocument-veiligheidsindex2014/6a74d3b9-3dcb-4e00-9747-e299f92a433a/>.
- [3] Margit Averdijk and Henk Elffers. The discrepancy between survey-based victim accounts and police reports revisited. *International Review of Victimology*, 18(2):91–107, 2012. ISSN 0269-7580. doi: 10.1177/0269758011432955.
- [4] Michael D. M. Bader, Stephen J. Mooney, Blake Bennett, and Andrew G. Rundle. The promise, practicalities, and perils of virtually auditing neighborhoods using google street view. *The ANNALS of the American Academy of Political and Social Science*, 669(1):18–40, 2017. ISSN 0002-7162. doi: 10.1177/0002716216681488.
- [5] Geoff Boeing. Osmnx: New methods for acquiring, constructing, analyzing, and visualizing complex street networks. *Computers, Environment and Urban Systems*, 65:126–139, 2017. ISSN 0198-9715. doi: 10.1016/j.comenvurbsys.2017.05.004. URL <http://arxiv.org/pdf/1611.01890>.
- [6] J. Boers. *Angst en vertrouwen. Het effect van positieve en negatieve factoren op veiligheidsbeleving*. Number 8 in Reeks Dynamics of Governance. Vrije Universiteit, 2008. ISBN 9789078223085.
- [7] Barbara B. Brown and Irwin Altman. Territoriality, defensible space and residential burglary: An environmental analysis. *Journal of Environmental Psychology*, 3(3):203–220, 1983. ISSN 0272-4944. doi: 10.1016/s0272-4944(83)80001-2.
- [8] Andrea Cohen, Alexander Gerhard Schwing, and Marc Pollefeys. Efficient structured parsing of facades using dynamic programming. In *2014 IEEE Conference on Computer Vision and Pattern Recognition*. IEEE, 2014. doi: 10.1109/cvpr.2014.410.
- [9] Andrea Cohen, Martin R. Oswald, Yanxi Liu, and Marc Pollefeys. Symmetry-aware façade parsing with occlusions. In *2017 International Conference on 3D Vision (3DV)*. IEEE, 2017. doi: 10.1109/3dv.2017.00052.
- [10] Paul Cozens and D. Hillier. *Revisiting Jane Jacobs's 'eyes on the street' for the twenty-first century: Evidence from environmental criminology*, pages 196–214. Routledge, 2012. ISBN 9780203095171. doi: 10.4324/9780203095171.
- [11] Paul Cozens and Terence Love. A review and current status of crime prevention through environmental design (cpted). *Journal of Planning Literature*, 30(4):393–412, 2015. ISSN 0885-4122. doi: 10.1177/0885412215595440.
- [12] Timothy D. Crowe. *Crime prevention through environmental design: applications of architectural design and space management concepts*. Butterworth-Heinemann, Boston, Mass, 2nd ed edition, 2000. ISBN 9780750671989.
- [13] Marco De Nadai, Yanyan Xu, Emmanuel Letouzé, Marta C. González, and Bruno Lepri. Socio-economic, built environment, and mobility conditions associated with crime: a study of multiple cities. *Scientific Reports*, 10(1), 2020. ISSN 2045-2322. doi: 10.1038/s41598-020-70808-2.
- [14] Balázs Dukai, Hugo Ledoux, and JE Stoter. A multi-height lod1 model of all buildings in the netherlands. *ISPRS Annals of Photogrammetry, Remote Sensing and Spatial Information Sciences*, 4(4/W8), 2019.

- [15] John Femiani, Wamiq Reyaz Para, Niloy Mitra, and Peter Wonka. Facade segmentation in the wild. 2018.
- [16] Sarah Foster, Billie Giles-Corti, and Matthew Knuiman. Creating safe walkable streetscapes: Does house design and upkeep discourage incivilities in suburban neighbourhoods? *Journal of Environmental Psychology*, 31(1):79–88, 2011. ISSN 0272-4944. doi: 10.1016/j.jenvp.2010.03.005.
- [17] Raghudeep Gadde, Renaud Marlet, and Nikos Paragios. Learning grammars for architecture-specific facade parsing. *International Journal of Computer Vision*, 117(3):290–316, 2016. ISSN 0920-5691. doi: 10.1007/s11263-016-0887-4. URL <https://hal.inria.fr/hal-01069379v2/document>.
- [18] Ernest Greene and Scott C. Fraser. Observation distance and recognition of photographs of celebrities' faces. *Perceptual and Motor Skills*, 95(2):637–651, 2002. ISSN 0031-5125. doi: 10.2466/pms.2002.95.2.637.
- [19] Antonin Guttman. R-trees. *ACM SIGMOD Record*, 14(2):47–57, 1984. ISSN 0163-5808. doi: 10.1145/971697.602266.
- [20] A M J Hulsebosch, H Elffers, W M E H Beijers, and C C J H Bijleveld. De veiligheidsindex amsterdam : Een quickscan naar de methodologische kwaliteit, het gebruik en de waardering van het instrument in de politieregio amsterdam- amstelland. Technical report, Strafrecht & Criminologie; Vrije Universiteit, 2008.
- [21] Mohamed R. Ibrahim, James Haworth, and Tao Cheng. Understanding cities with machine eyes: A review of deep computer vision in urban analytics. *Cities*, 96:102481, 2020. ISSN 0264-2751. doi: <https://doi.org/10.1016/j.cities.2019.102481>. URL <http://www.sciencedirect.com/science/article/pii/S0264275119308443>.
- [22] Jane Jacobs. *The Death and Life of Great American Cities*. 1961. ISBN 0394421590 9780394421599 067974195X 9780679741954.
- [23] Marloes De Jong, Willem A. Wagenaar, Gezinus Wolters, and Ilse M. Verstijnen. Familiar face recognition as a function of distance and illumination: a practical tool for use in the courtroom. *Psychology, Crime and Law*, 11(1):87–97, 2005. ISSN 1068-316X. doi: 10.1080/10683160410001715123.
- [24] Gefei Kong and Hongchao Fan. Enhanced facade parsing for street-level images using convolutional neural networks. *IEEE Transactions on Geoscience and Remote Sensing*, pages 1–13, 2020. ISSN 0196-2892. doi: 10.1109/tgrs.2020.3035878.
- [25] Filip Korč and Wolfgang Förstner. eTRIMS image database for interpreting images of man-made scenes. 2009.
- [26] Mateusz Kozinski, Raghudeep Gadde, Sergey Zagoruyko, Guillaume Obozinski, and Renaud Marlet. A mrf shape prior for facade parsing with occlusions. In *2015 IEEE Conference on Computer Vision and Pattern Recognition (CVPR)*. IEEE, 2015. doi: 10.1109/cvpr.2015.7298899.
- [27] Mateusz Koziński, Guillaume Obozinski, and Renaud Marlet. *Beyond Procedural Facade Parsing: Bidirectional Alignment via Linear Programming*, pages 79–94. Springer International Publishing, 2015. ISBN 0302-9743. doi: 10.1007/978-3-319-16817-3_6.
- [28] Samuel H. Langton and Wouter Steenbeek. Residential burglary target selection: An analysis at the property-level using google street view. *Applied Geography*, 86:292–299, 2017. ISSN 0143-6228. doi: 10.1016/j.apgeog.2017.06.014.
- [29] Inhye Lee, Sungwon Jung, Jaewook Lee, and Elizabeth Macdonald. Street crime prediction model based on the physical characteristics of a streetscape: Analysis of streets in low-rise housing areas in south korea. *Environment and Planning B: Urban Analytics and City Science*, 46(5):862–879, 2017. ISSN 2399-8083. doi: 10.1177/2399808317735105. URL <https://doi.org/10.1177/2399808317735105>.
- [30] Chuan-Kang Li, Hong-Xin Zhang, Jia-Xin Liu, Yuan-Qing Zhang, Shan-Chen Zou, and Yu-Tong Fang. Window detection in facades using heatmap fusion. *Journal of Computer Science and Technology*, 35(4):900–912, 2020. doi: 10.1007/s11390-020-0253-4. URL http://jcst.ict.ac.cn/CN/abstract/article_2660.shtml.

- [31] R. C. Lindsay, C. Semmler, N. Weber, N. Brewer, and M. R. Lindsay. How variations in distance affect eyewitness reports and identification accuracy. *Law Hum Behav*, 32(6):526–35, 2008. ISSN 0147-7307. doi: 10.1007/s10979-008-9128-x.
- [32] Hantang Liu, Yinghao Xu, Jialiang Zhang, Jianke Zhu, Yang Li, and Steven C. H. Hoi. Deepfacade: A deep learning approach to facade parsing with symmetric loss. *IEEE Transactions on Multimedia*, 22(12):3153–3165, 2020. ISSN 1520-9210. doi: 10.1109/tmm.2020.2971431.
- [33] Geoffrey R. Loftus and Erin M. Harley. Why is it easier to identify someone close than far away? *Psychonomic Bulletin and Review*, 12(1):43–65, 2005. ISSN 1069-9384. doi: 10.3758/bf03196348.
- [34] Wenguang Ma and Wei Ma. Deep window detection in street scenes. *KSII Transactions on Internet and Information Systems*, 14(2), 2020. ISSN 19767277. doi: 10.3837/tiis.2020.02.022.
- [35] Julia E. Macdonald and Robert Gifford. Territorial cues and defensible space theory: The burglar's point of view. *Journal of Environmental Psychology*, 9(3):193–205, 1989. ISSN 0272-4944. doi: 10.1016/s0272-4944(89)80034-9.
- [36] Carla. L. Maclean, C.A. Elizabeth Brimacombe, Meredith Allison, Leora C. Dahl, and Helena Kadlec. Post-identification feedback effects: Investigators and evaluators. *Applied Cognitive Psychology*, 25(5):739–752, 2011. ISSN 0888-4080. doi: 10.1002/acp.1745.
- [37] Akkelies Nes and Manuel Lopez. Macro and micro scale spatial variables and the distribution of residential burglaries and theft from cars: An investigation of space and crime in the dutch cities of alkmaar and gouda. *The Journal of Space Syntax*, 1:296–314, 2010.
- [38] Oscar Newman. *Defensible Space*. Macmillan New York, 1972. ISBN 0851391362.
- [39] Candice L. Odgers, Avshalom Caspi, Christopher J. Bates, Robert J. Sampson, and Terrie E. Moffitt. Systematic social observation of children's neighborhoods using google street view: a reliable and cost-effective method. *Journal of Child Psychology and Psychiatry*, 53(10):1009–1017, 2012.
- [40] M.P. Peeters and T. Vander Beken. The relation of cptd characteristics to the risk of residential burglary in and outside the city center of ghent. *Applied Geography*, 86:283–291, 2017. ISSN 0143-6228. doi: 10.1016/j.apgeog.2017.06.012.
- [41] Sihang Qiu, Achilleas Psyllidis, Alessandro Bozzon, and Geert-Jan Houben. Crowd-mapping urban objects from street-level imagery. In *The World Wide Web Conference on - WWW '19*. ACM Press, 2019. doi: 10.1145/3308558.3313651.
- [42] Danielle M. Reynald. Guardianship in action: Developing a new tool for measurement. *Crime Prevention and Community Safety*, 11(1):1–20, 2009. ISSN 1743-4629. doi: 10.1057/cpcs.2008.19. URL <https://doi.org/10.1057/cpcs.2008.19>.
- [43] Danielle M. Reynald. Factors associated with the guardianship of places: Assessing the relative importance of the spatio-physical and sociodemographic contexts in generating opportunities for capable guardianship. *Journal of Research in Crime and Delinquency*, 48(1):110–142, 2011. ISSN 0022-4278. doi: 10.1177/0022427810384138.
- [44] Danielle M. Reynald and Henk Elffers. The future of newman's defensible space theory. *European Journal of Criminology*, 6(1):25–46, 2009. ISSN 1477-3708. doi: 10.1177/1477370808098103.
- [45] H. Riemenschneider, U. Krispel, W. Thaller, M. Donoser, S. Havemann, D. Fellner, and H. Bischof. Irregular lattices for complex shape grammar facade parsing. In *2012 IEEE Conference on Computer Vision and Pattern Recognition*. IEEE, 2012. doi: 10.1109/cvpr.2012.6247857.
- [46] Dalit Shach-Pinsky. Measuring security in the built environment: Evaluating urban vulnerability in a human-scale urban form. *Landscape and Urban Planning*, 191:103412, 2019. ISSN 0169-2046. doi: 10.1016/j.landurbplan.2018.08.022.

- [47] Dalit Shach-Pinsky and Tamar Ganor. Security sensitivity index: evaluating urban vulnerability. *Proceedings of the Institution of Civil Engineers - Urban Design and Planning*, 168(3):115–128, 2015. doi: 10.1680/udap.13.00015. URL <https://www.icevirtuallibrary.com/doi/abs/10.1680/udap.13.00015>.
- [48] Shahin Sharifi Noorian, Sihang Qiu, Achilleas Psyllidis, Alessandro Bozzon, and Geert-Jan Houben. Detecting, classifying, and mapping retail storefronts using street-level imagery. In *Proceedings of the 2020 International Conference on Multimedia Retrieval*. ACM, 2020. doi: 10.1145/3372278.3390706.
- [49] Hao Sheng, Keniel Yao, and Sharad Goel. Surveilling surveillance: Estimating the prevalence of surveillance cameras with street view data. 2021.
- [50] United Nations Human Settlements Programme (UN-Habitat). United nations system-wide guidelines on safer cities and human settlements. Report, 2020. URL https://unhabitat.org/sites/default/files/2020/03/un_systemwide_guidelines_on_safer_cities_and_human_settlements.pdf.
- [51] Department of Economic United Nations and Population Division Social Affairs. World urbanization prospects 2018: Highlights. Report, 2019. URL <https://population.un.org/wup/Publications/Files/WUP2018-Highlights.pdf>.
- [52] S.J. Vergouw, R.P.W. Jennissen, G. Weijters, and P.R. Smit. Naar nationale veiligheidsindices, 2014 2014. URL <http://hdl.handle.net/20.500.12832/145>.
- [53] Jinglu Wang, Chun Liu, Tianwei Shen, and Long Quan. Structure-driven facade parsing with irregular patterns. In *2015 3rd IAPR Asian Conference on Pattern Recognition (ACPR)*. IEEE, 2015. doi: 10.1109/acpr.2015.7486462.
- [54] David Weisburd, Elizabeth R Groff, and Sue-Ming Yang. *The criminology of place: Street segments and our understanding of the crime problem*. Oxford University Press, 2012.